



Picosecond Photodetectors: What can we learn from modern III-V semiconductor technologies?

Serge Oktyabrsky

SUNY College of Nanoscale Science and Engineering, Albany NY



Outline

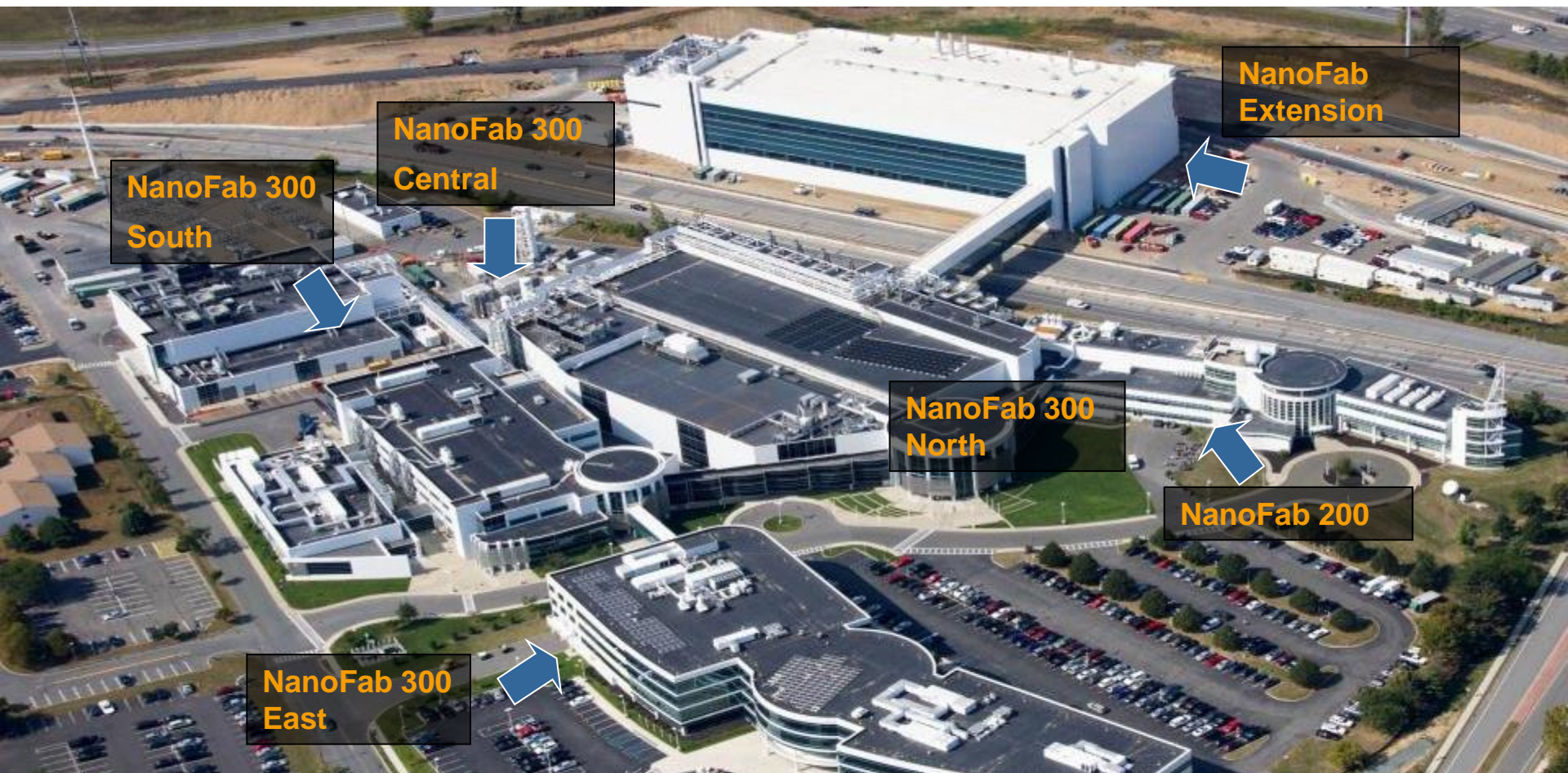
- CNSE brief overview
- Applications of ps UV photodetectors
- Vertical vs. Lateral field PDs
- Fast APDs
- How to make ps single-photoelectron counting detector?
- III-V technologies – challenges and breakthroughs
- Summary



CNSE OVERVIEW

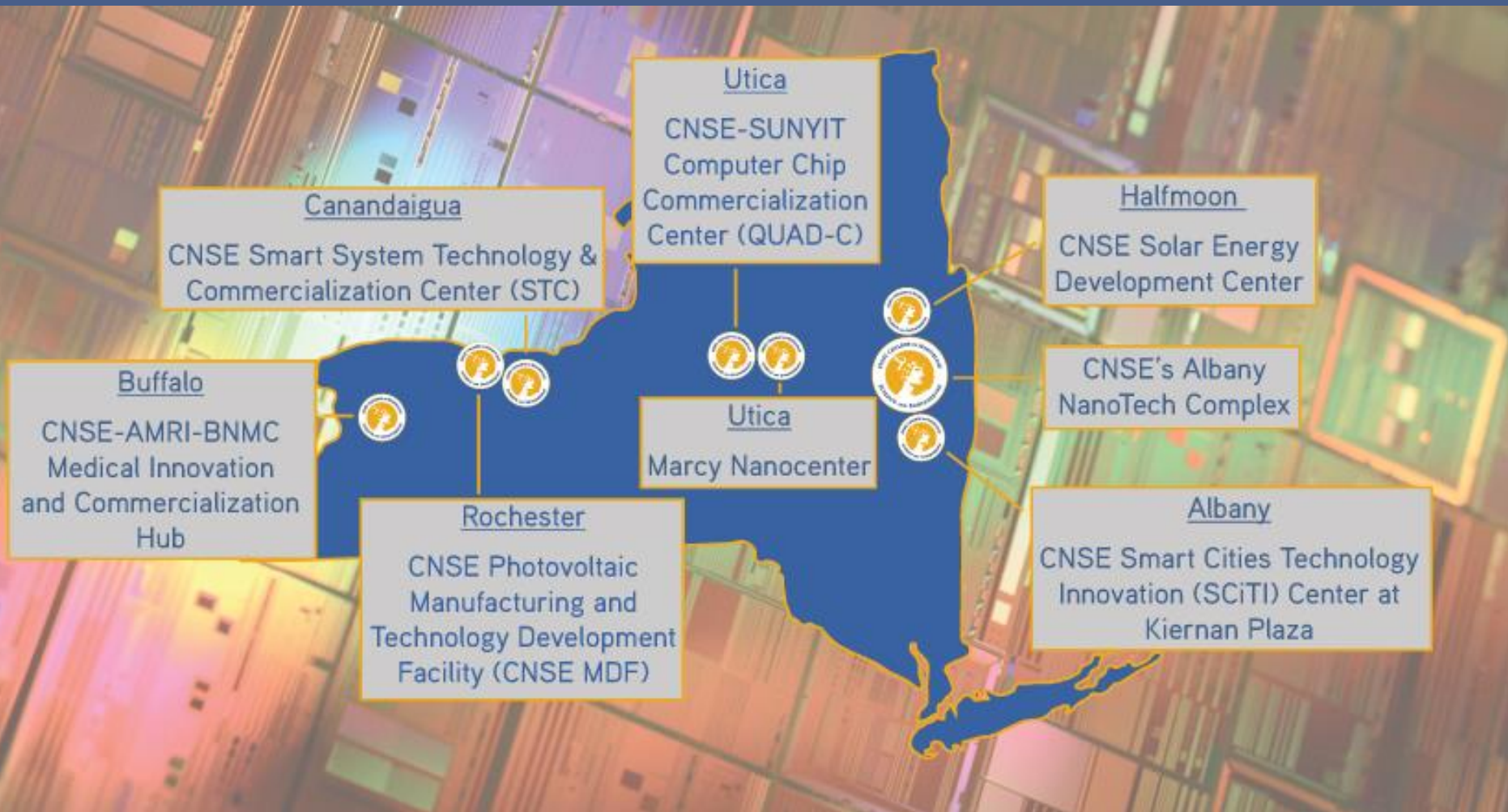
Mr. Ross Goodman, Esq.
Assistant Vice President, Business Development and
Economic Outreach
SUNY College of Nanoscale Science and Engineering

World Class Facilities



- ◆ > 1,000,000 sq.ft. of cutting-edge facilities, with 135,000 sq. ft. of 300mm and 450 mm cleanrooms with a current expansion to 1,300,000 sq. ft.
- ◆ More than 300 industry partners including electronics, energy, defense & biohealth
- ◆ Over \$17B investments and over 3,100 R&D jobs currently on site

CNSE's STATEWIDE NANO IMPACT



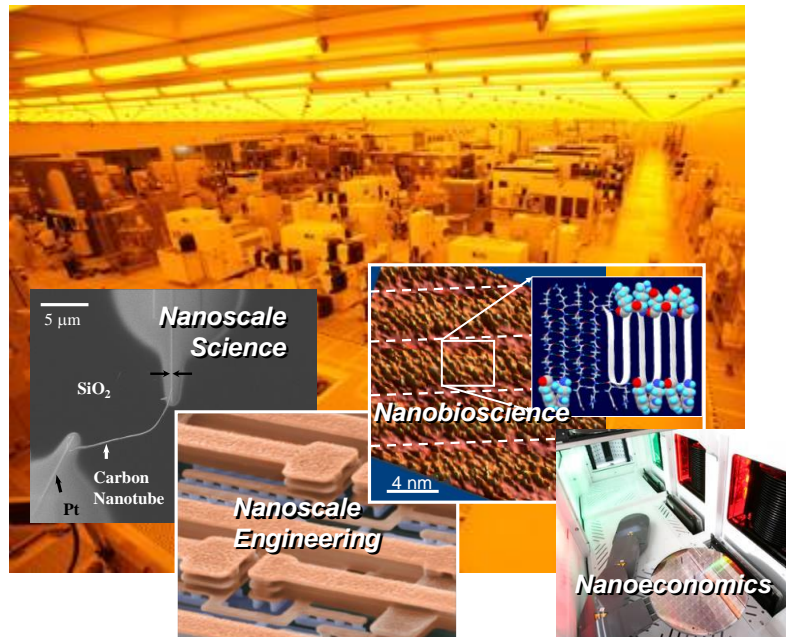


CNSE is dedicated to nanotechnology with constellations in:

- ◆ **Nanoscience**
- ◆ **Nanoengineering**
- ◆ **Nanobioscience**
- ◆ **Nanoeconomics**

Vision Leverage combined resources to establish effective partnerships that will enable realization of *industry* technology roadmaps and pioneering nanoscale research.

Mission Create a financially and technically competitive environment to empower the nanoelectronics *industry* with manufacturing advantages through vertically integrated partnerships.





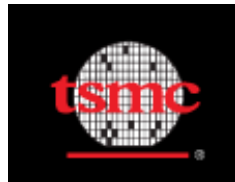
NYS Governor Cuomo Announces Global 450 Consortia

- \$4.8 billion investment
 - \$4.4 billion pledged by IBM, Intel, TSMC, GlobalFoundries, Samsung
 - \$400 million pledged by NYS
- Intel to establish its East Coast headquarters in Albany to manage 450nm development.

R&D in Albany, Canandaigua, Utica, East Fishkill and Yorktown Heights.

2,700 new high-tech jobs, including:

- 800 at the CNSE
- 400 in Utica
- 1,500 construction jobs in Albany



CNSE Site Expansion



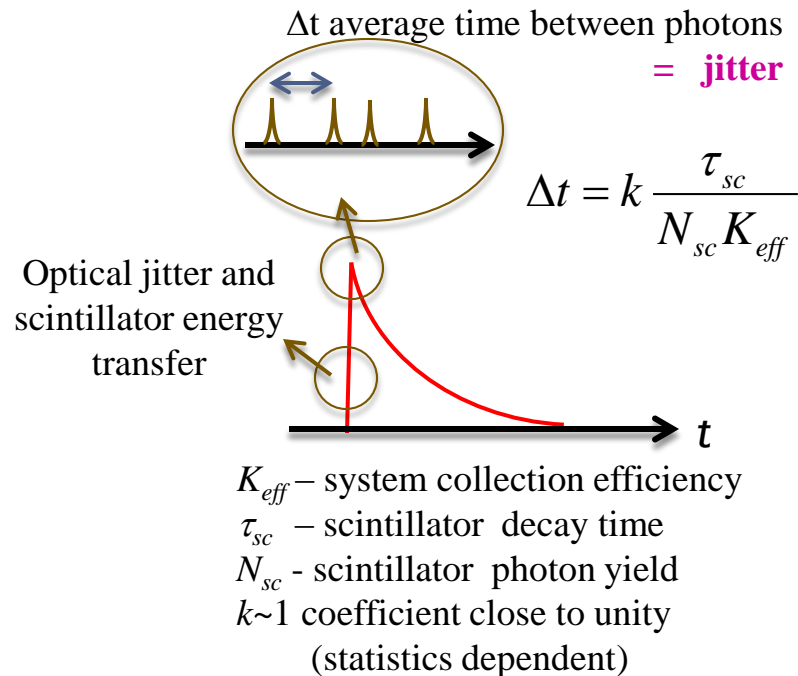


Picosecond near UV Semiconductor Photodetectors : Applications

Applications for ultra-fast UV photodetectors:

- High energy physics
 - LAr and LXe detectors
 - Fast crystal calorimetry: many inorganic scintillators, i.e. BaF₂, emit in UV
 - Cherenkov detectors
- Space research
- Medical TOF imaging and tomography
 - TOF positron emission tomography
 - Fast gamma imaging/ TOF tomography

Scintillator emission



Example: Projected time resolution for TOF PET

Need: Semiconductor
UV/Vis single photoelectron
detector with ps resolution

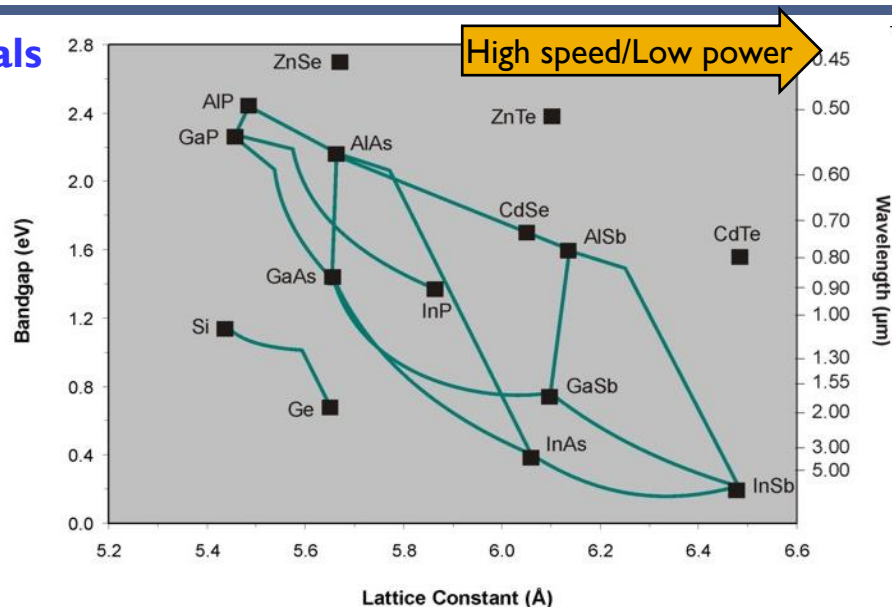
	Decay time (ns)	Light output (ph./MeV)	Δt at $K_{eff}=0.2$ & 0.5 MeV (ps)
LYSO	40	40,000	10
BaF ₂ (fast component)	0.9	1400	6
LaBr ₃ (Ce)	16	70,000	3
CsBr	0.07	20	35



Materials: Bulk Properties

Group III-V materials

Group 2a	Group 3a	Group 4a	Group 5a	Group 6a
4 Be Beryllium 9.0122	5 B Boron 10.811	6 C Carbon 12.011	7 N Nitrogen 14.0067	8 O Oxygen 15.9994
12 Mg Magnesium 24.305	13 Al Aluminum 26.9815	14 Si Silicon 28.086	15 P Phosphorus 30.9738	16 S Sulfur 32.066
30 Zn Zinc 65.39	31 Ga Gallium 69.72	32 Ge Germanium 72.61	33 As Arsenic 74.9216	34 Se Selenium 78.96
48 Cd Cadmium 112.41	49 In Indium 114.82	50 Sn Tin 118.71	51 Sb Antimony 121.76	52 Te Tellurium 127.60
80 Hg Mercury 200.59	81 Tl Thallium 204.38	82 Pb Lead 207.2	83 Bi Bismuth 208.98	84 Po Polonium (210)



Attractive material
parameters are
similar for
MOSFETs and
ultrafast PDs

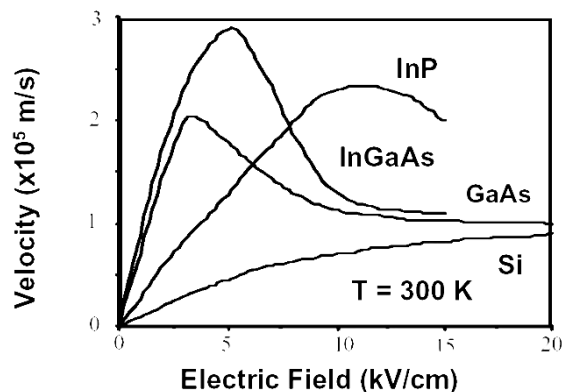
300 K Electron Transport Properties

300 K Hole Transport Properties

	E_g , eV	$m_{e(-)}$	$m_{e(-)}$	μ_e , cm ² /Vs	$V_{e,sat}$, 10 ⁷ cm/s	m_{hh}	m_{lh}	m_{hh-in_pl}	μ_h , cm ² /Vs
Si	1.12	0.19	0.98	1350	0.7	0.54	0.15	0.22	460
Ge	0.66	0.082	1.64	3900	0.7	0.34	0.043	0.057	1900
GaAs	1.42	0.067	-	8500	2	0.53	0.08	0.11	400
InP	1.35	0.079	-	5900	2.4	0.56	0.12	0.16	150
In _{0.53} GaAs	0.8	0.04	-	14000	2.9	0.36	0.041	0.052	400
InAs	0.36	0.027	-	33000	3.5	0.4	0.026	0.035	450
GaSb	0.73	0.041	-	3750		0.8	0.05	0.055	680
InSb	0.17	0.013	-	77000	5.0	0.42	0.016	0.020	850



Drift velocity

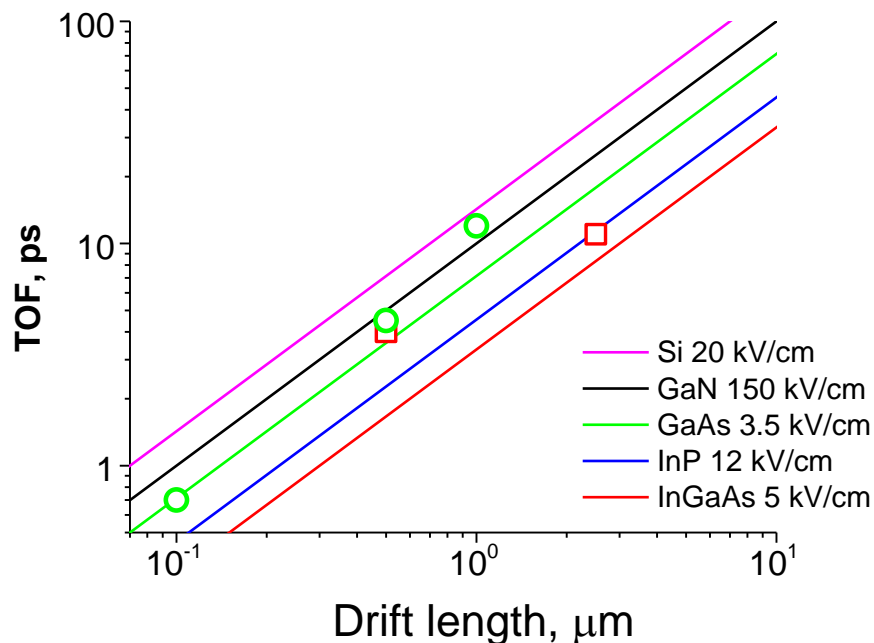


Saturation velocity and necessary operating voltage for 10ps risetime

Material	Saturation field, kV/cm	Spacing for 10ps, μm	Operating Voltage, V
Si	20	0.7	1.4
GaN	150	1.4	21*
GaAs	3.5	2	0.7
InP	12	2.3	2.6
InGaAs	5	3	1.5

* For GaN operating voltage should be further increased due to longer absorption lengths and lower mobility

Saturation velocity – limited electron drift time (TOF)

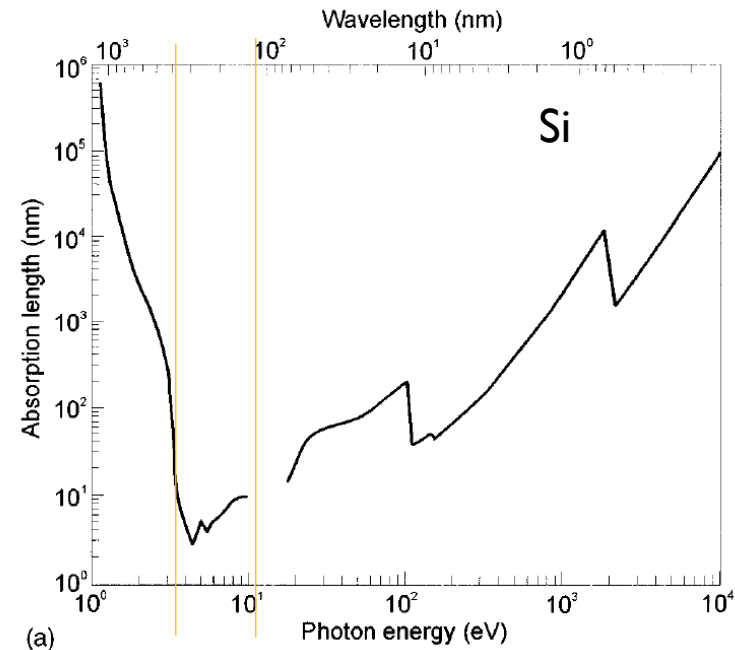
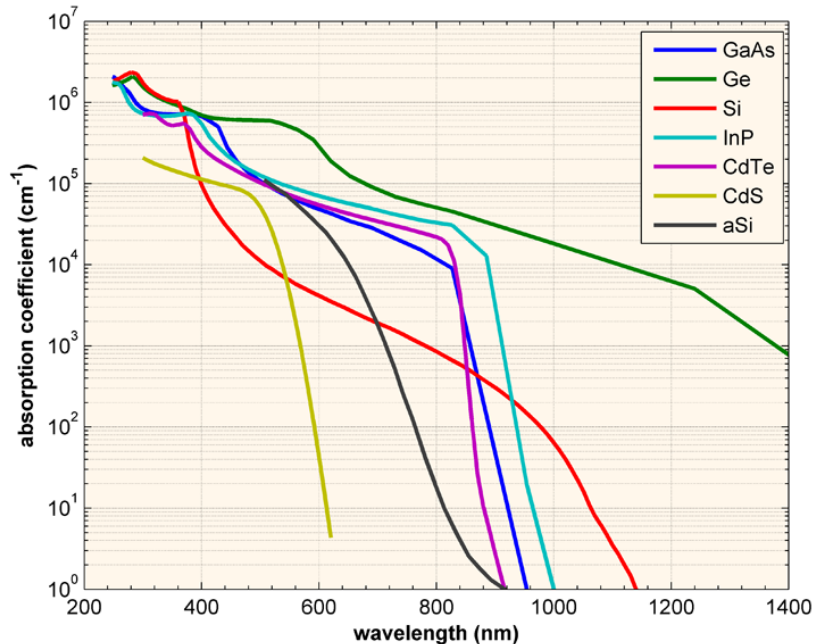


Experimental data from:

III-V MSMs (lateral field): Ralph 1992, Zeghbroeck 1988, Chou 1992, Gallo 2013,



Absorption coefficients in semiconductors [Carruthers, Electro-Optics Handbook]

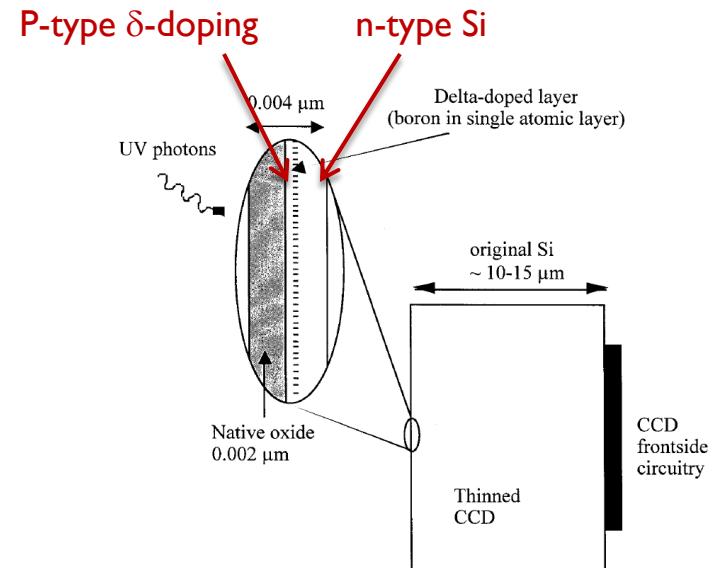
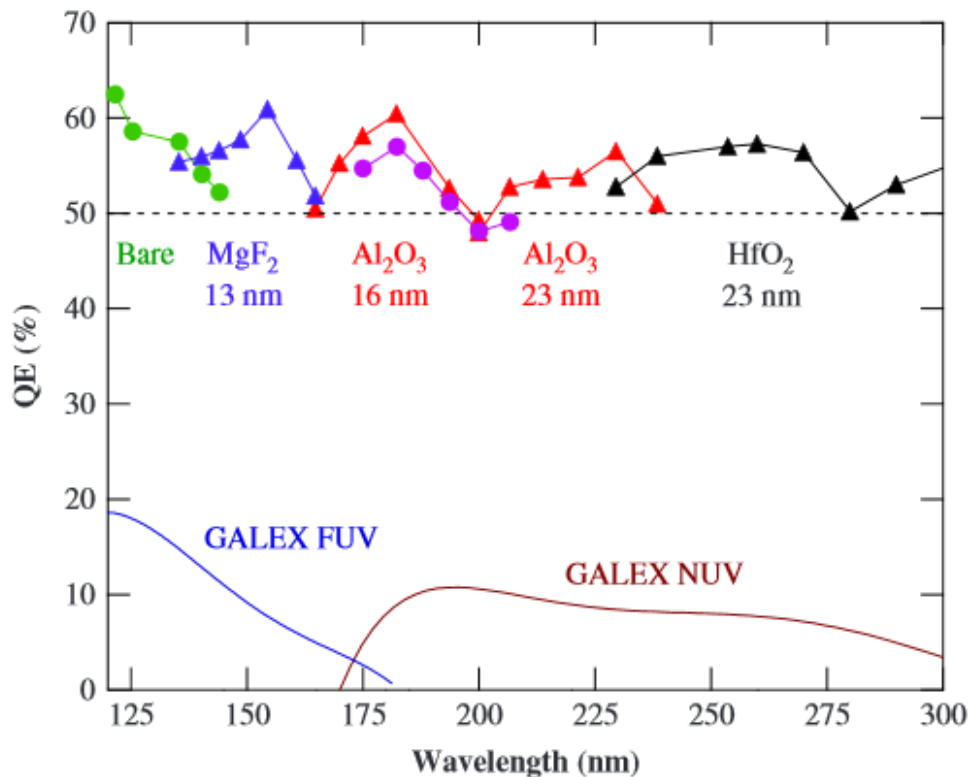


- In the region $\lambda < 360\text{nm}$ the absorption takes place within $< 100\text{ \AA}$
- Highly-doped layer in p-i-n or APD structures kills efficiency
- Evolution of carriers is strongly affected by the surface/interface recombination, relaxation in the Brillouin zone close to the surface
- Si has the highest α in UV and the lowest in visible \rightarrow the worst material for fast PDs
- Detectors with **lateral field** are of great interest for (near)-UV



Quantum efficiency of UV-enhanced (delta-doped) CCDs 4x4 μm^2 pixel [JPL]

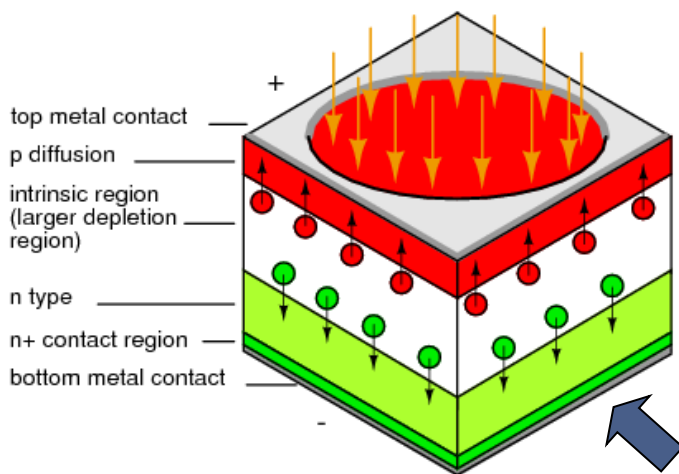
Nikzad et al. Appl. Optics **51** 365(2012); Proc. SPIE **2198** 907 (1994).



- Making a thin inversion layer increases UV efficiency but also increases sheet resistance
- Sheet resistance is high $\sim 10 \text{ k}\Omega/\text{sq}$.
- Fine in slow devices, but series resistance kills leading front

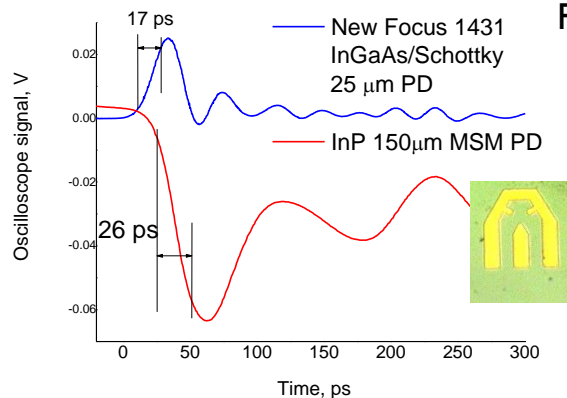


Geometry: Lateral vs. Vertical



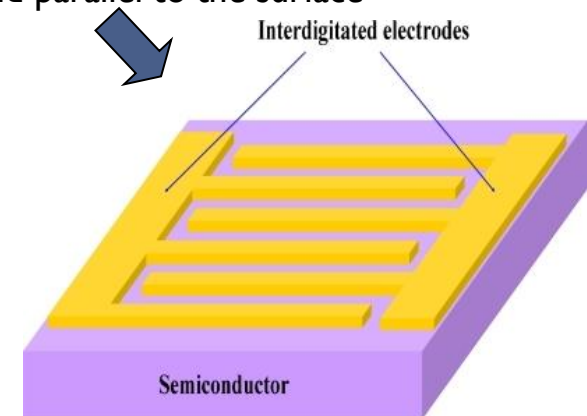
Vertical:

Top and bottom contacts
Field normal to the surface



Lateral:

Both contacts on one surface
Field parallel to the surface



Vertical (p-i-n)

Large area contact, usually thin depletion layer, higher C

Surface dead layer due to top contact, bad for UV

3D device, requires special packaging

Most common semiconductor detector type

Lateral (MSM)

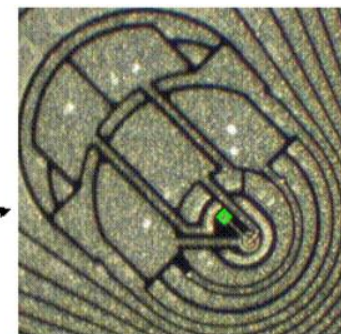
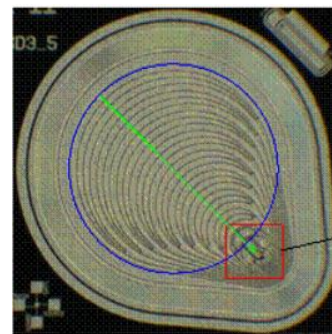
Small area contact, large gaps between electrodes, lower C

No dead layer, large exposed surface, surface recombination

Planar device, compatible with FET process, simple integration

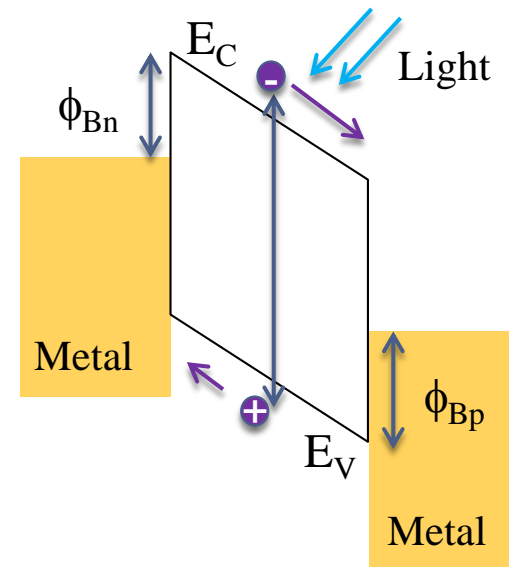
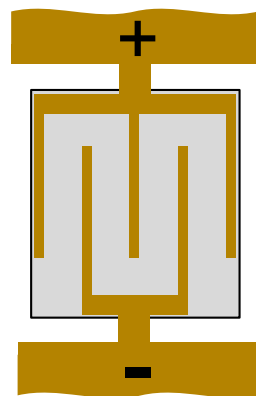
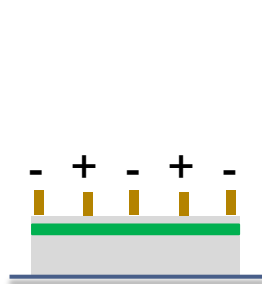
Some designs commercially available, e.g. MSM's or Si drift detectors

Silicon Drift Detector with integrated transistor [from PulseTor.com]





- The simplest lateral field detector is MSM structure which is back-to-back connected Schottky diodes



Advantages

- Low capacitance per unit area
- Lack of dead contact layer (important to absorption coefficients $\alpha > 10^6 \text{ cm}^{-1}$ \rightarrow 10nm absorption length)
- Reduced volume for generation-related dark current (in particular QW structures)
- Planarity, compatibility with FET process flow

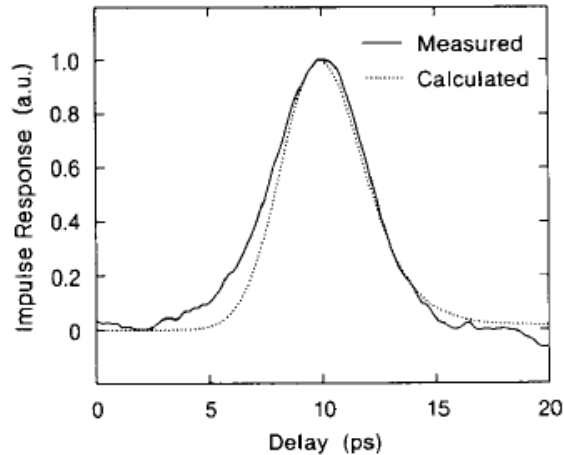
Disadvantages

- Reflection from surface metal contacts
- Surface states enhance generation/recombination, reduce efficiency and increase dark current
- Metal-semiconductor interface is the origin of traps and leakage

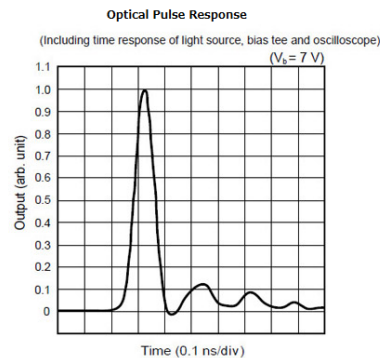


Zeghbroeck et al. , EDL 1988

GaAs MSM: 105 GHz, 5 ps (drift limited)

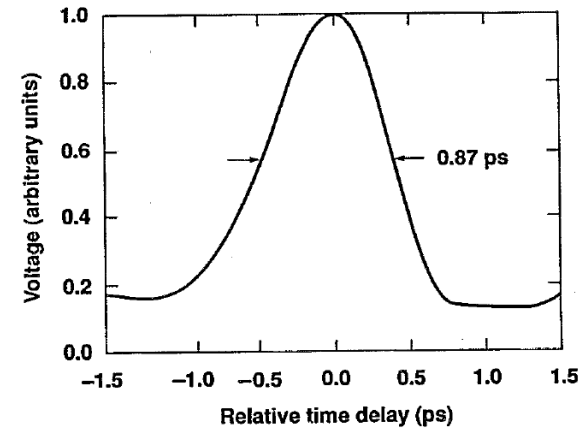


Hamamatsu GaAs MSM
30 ps FWHM

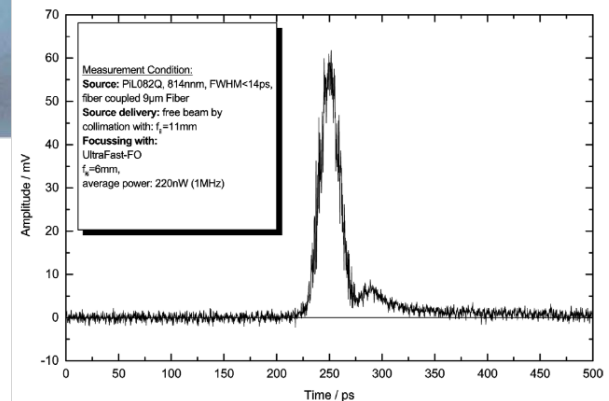


Chou et al. , APL 1992

LT-GaAs MSM: 0.87ps



Advanced Laser Diode Systems
InGaAs MSM: 20ps FWHMz



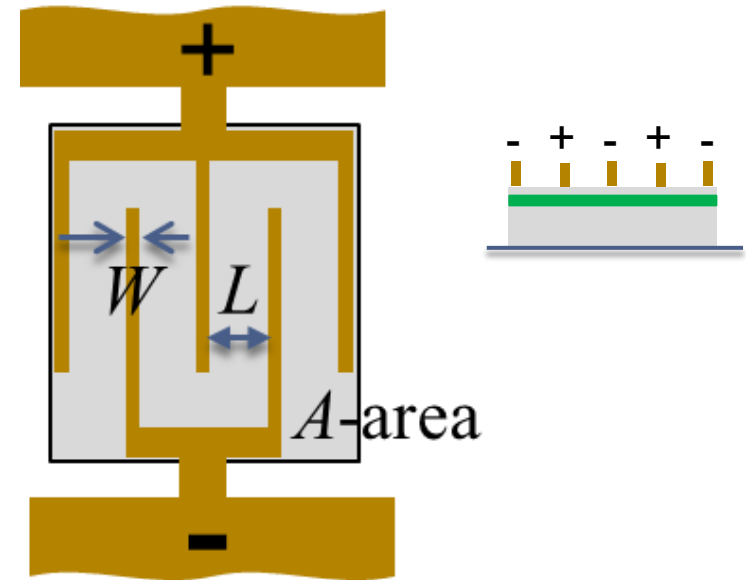
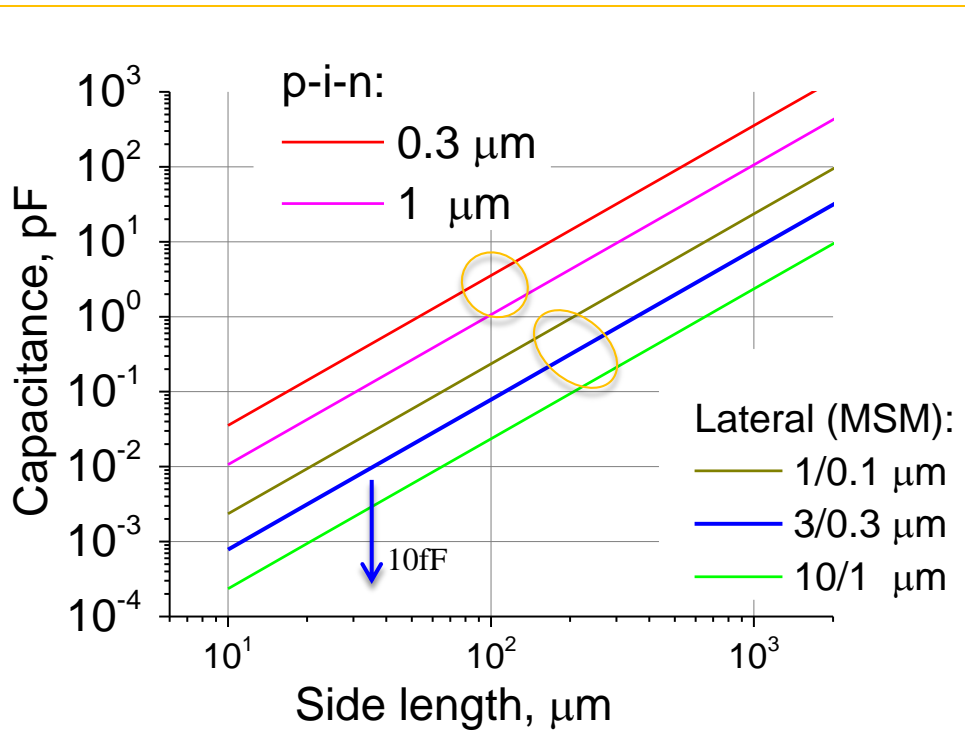


MSM PD: Capacitance

Capacitance of MSM device:

$$C = \frac{K(k)}{K(\sqrt{1-k^2})} \frac{\epsilon_0(\epsilon+1)A}{4(L+W)}$$

$$K(k) = \int_0^{\pi/2} \frac{d\phi}{\sqrt{1-k^2 \sin^2 \phi}}$$
$$k = \tan^2 \frac{\pi W}{4(L+W)}$$



- MSM shows ~5x reduction of device capacitance (vs. pin) for the same drift length
- Capacitance reduction for the same TOF*: 15x as compared to Si p-i-n.

*TOF- Electron time-of-flight or drift time



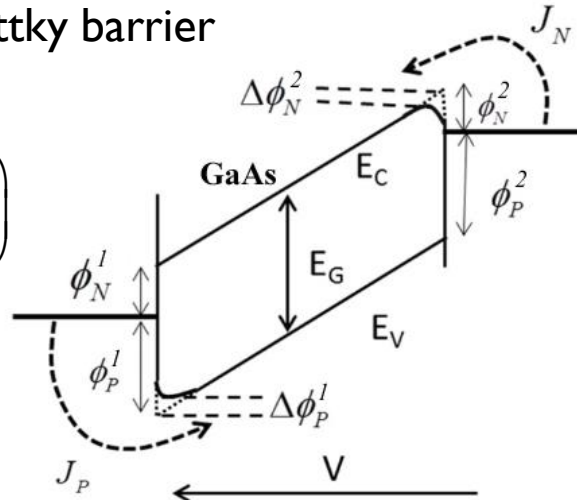
Dark current

- Shot noise is the major intrinsic noise source

$$\langle i_{PD_noise}^2 \rangle = \left(2qI_{tot} + \frac{4kT}{R_{eq}} \right) \Delta f \xrightarrow{\text{small signal}} 2qI_{dark} \Delta f$$

- Dark current in MSM is mostly due to thermionic emission over the Schottky barrier

$$J_{thermionic} \sim T^2 \exp\left(-\frac{q\phi_B}{kT}\right)$$



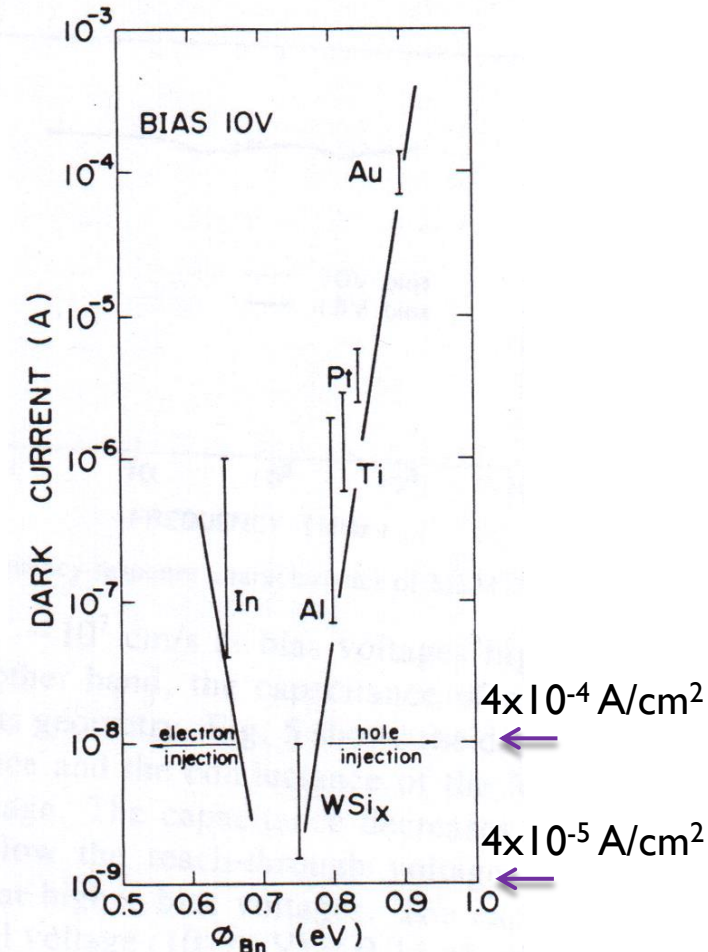
- Use of a contact on higher bandgap semiconductor (AlGaAs or AlInAs) lowers the dark current
- The lowest dark current in InAlAs/InGaAs heterostructure

$4.5 \times 10^{-6} \text{ A/cm}^2$ [Kim et al. TED 51 351 (2004)]

- Compare to $5 \times 10^{-11} \text{ A/cm}^2$ for Si p-i-n PDs

Dark current in GaAs MSM

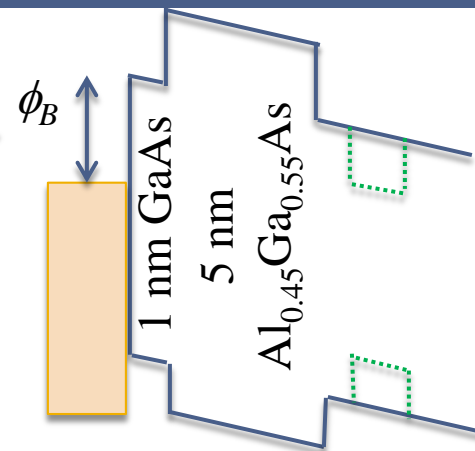
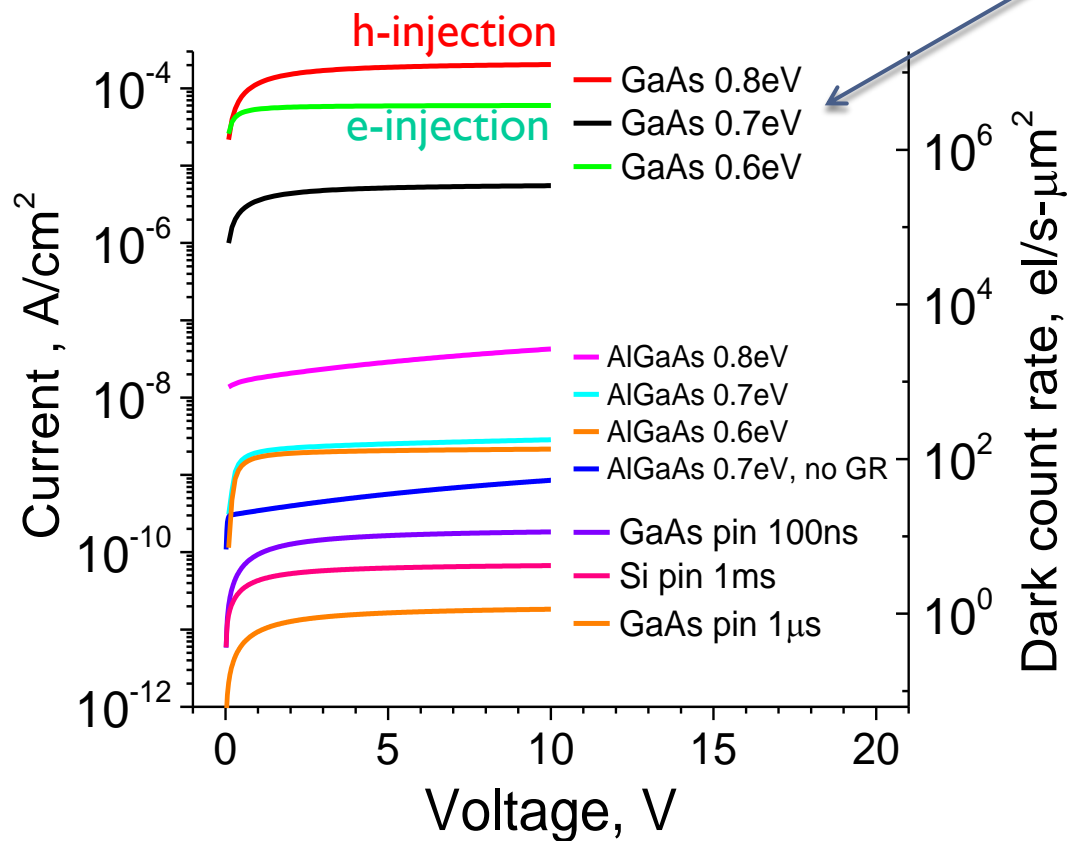
[Ito et al. JQE 22 1073 (1986)]





Dark current

Dark current in 1 μ m GaAs MSM and p-i-n diodes: effect of thermionic emission and generation



- A simple built-in heterojunction barrier close to Schottky contact can reduce current by 3-4 orders of magnitude to ~ 100 el/s- μ m²
- It can be further reduced by introducing p-n junctions instead of Schottky junctions
- Feasible to have one heterojunction and another Schottky junction
- Then dark current is limited by generation current:

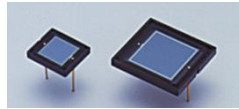
$$I_{SHR} = qV_{depletion} \frac{n_i}{2\tau_o}$$



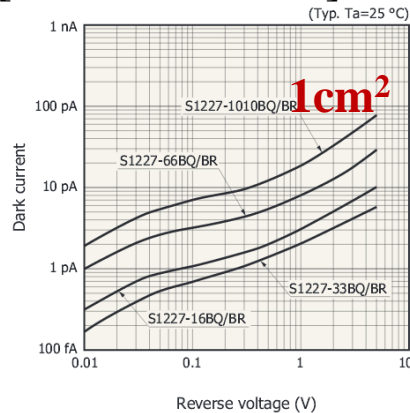
Dark currents in p-i-n PDs

Dark current in Si p-i-n PD

SI227 series [hamamatsu.com]

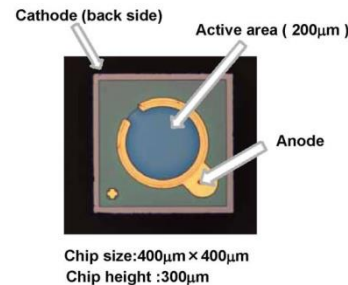


Dark current
= 0.1 nA/cm²

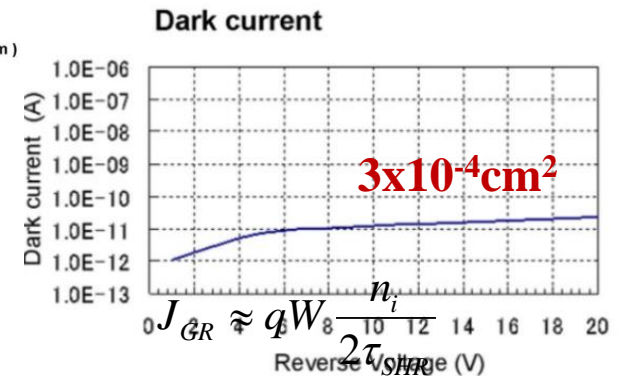


Dark current in GaAs p-i-n PD

[kyosemi.co.jp]



30 nA/cm²



Generation dark current in W=0.5 μm pin diodes

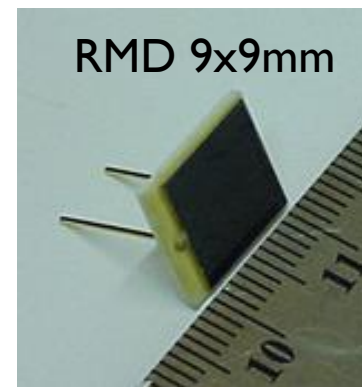
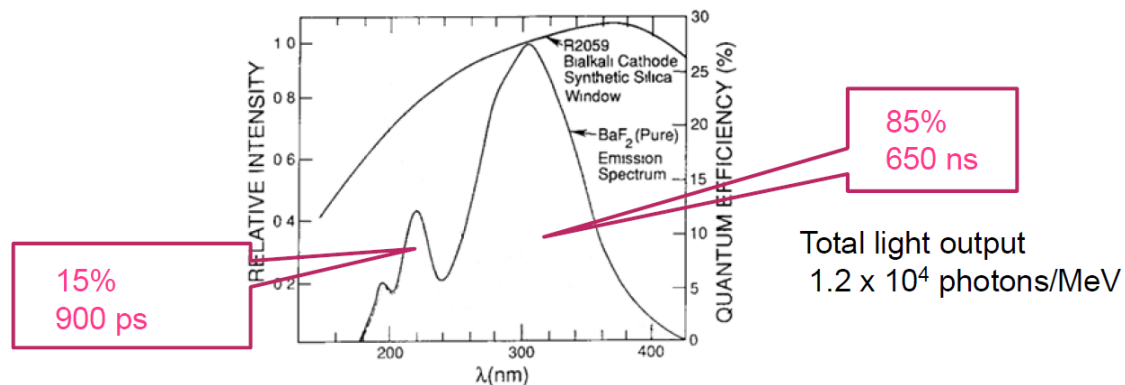
Material	n_i, cm^{-3}	τ_{SHR}, s	$J_{GR}, \text{A/cm}^2$
Si	1.5×10^{10}	10^{-3}	6×10^{-11}
GaAs	1.8×10^6	10^{-8}	7×10^{-10}
$\text{Al}_{0.3}\text{GaAs}$	1.7×10^3	10^{-10}	7×10^{-11}

- Reverse current is ~2 orders of magnitude higher in GaAs than in Si p-i-n's
- There are number of reports of lower reverse currents, i.e. ~50 pA/cm² in p⁺-p-n⁺ [Chen et al. J. Phys.D, 44 215303 (2011)]
- Generation current is scaling as volume of the depletion region. Effective volume can be reduced in lateral structure

$$J_{GR} \approx qW \frac{n_i}{2\tau_{SHR}}$$

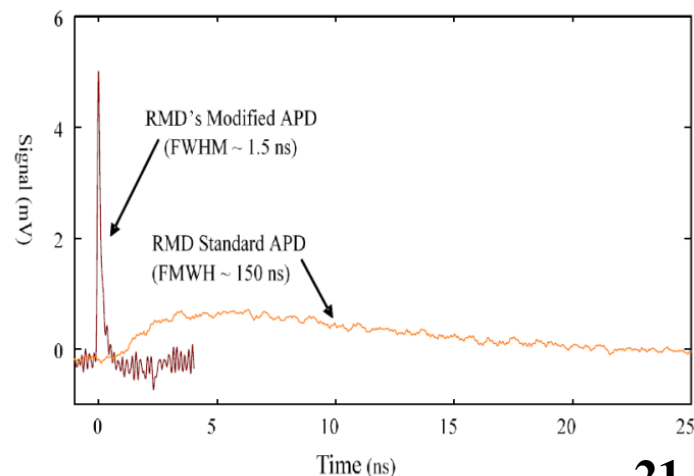
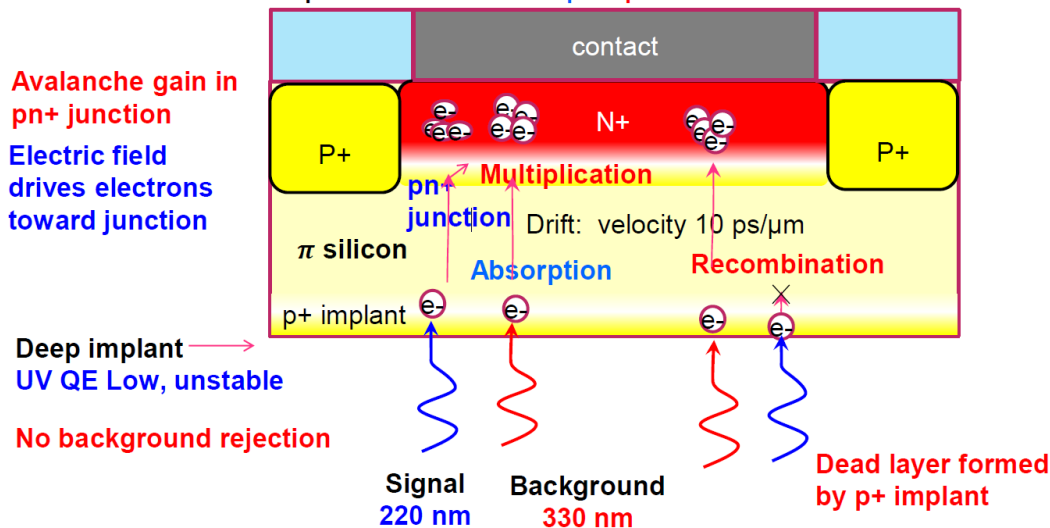


From D. Hitlin, CalTech/RMD/JPL, 2013



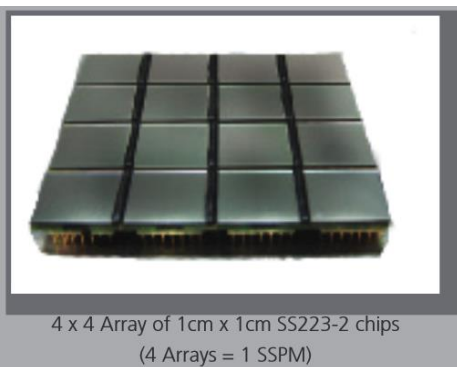
Reach-Through Avalanche Photodiode (RTAPD)

Reverse biased photodiode with $p^+ \pi p n^+$ structure

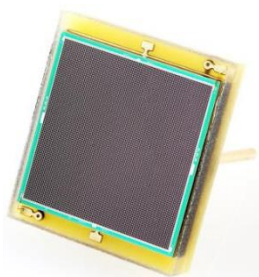


Next step: Sensor Partitioning

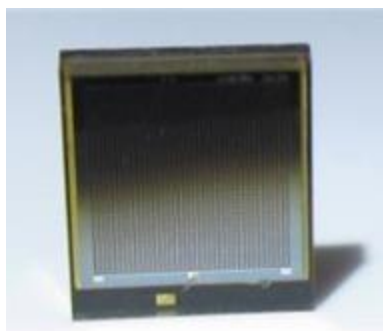
RMD SSPM: 130 fF/pixel
(pixel size $\sim 50\mu\text{m}$)



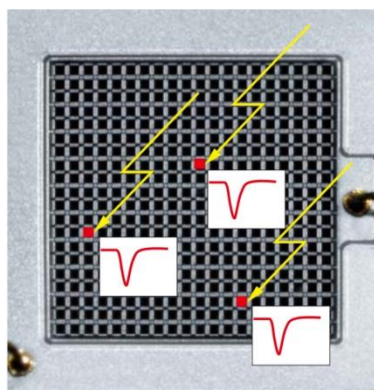
KETEC SSPM



AdvanSiD SSPM

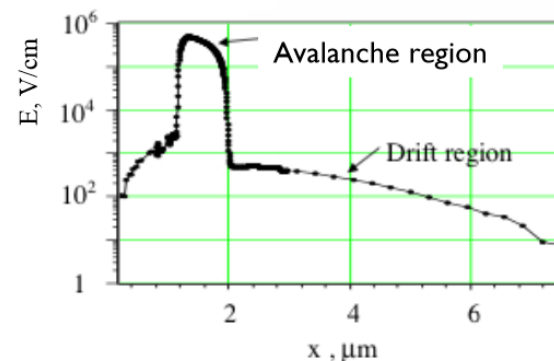
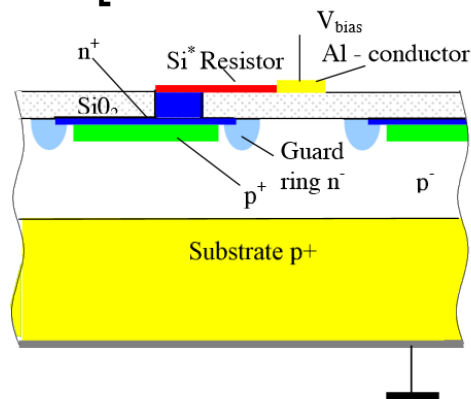


Hamamatsu SSPM:



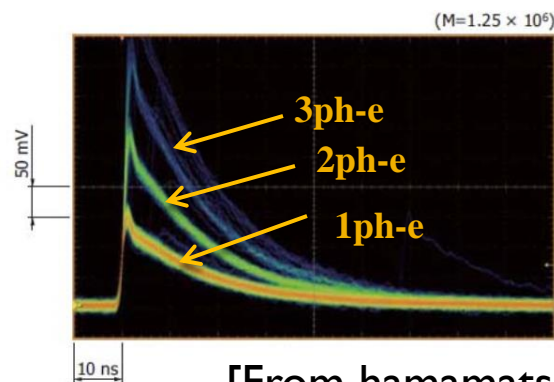
SSPM: APD array in parallel

[From: "Scintillation Detectors", U. of Heidelberg]



- Geiger-mode: Gain $\sim 10^6$
- ns-range device: best jitter $\sim 100\text{ps}$

S12571



[From hamamatsu.com]

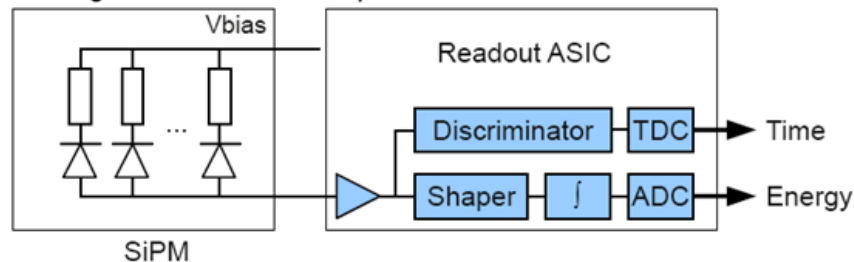


Philips Digital SSPM

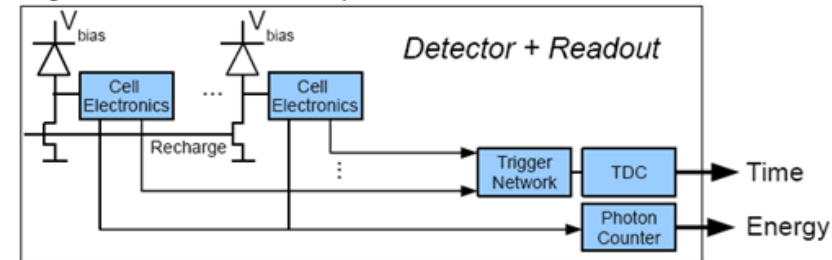
[From: www.research.philips.com and
PDPC presentation, 2012]



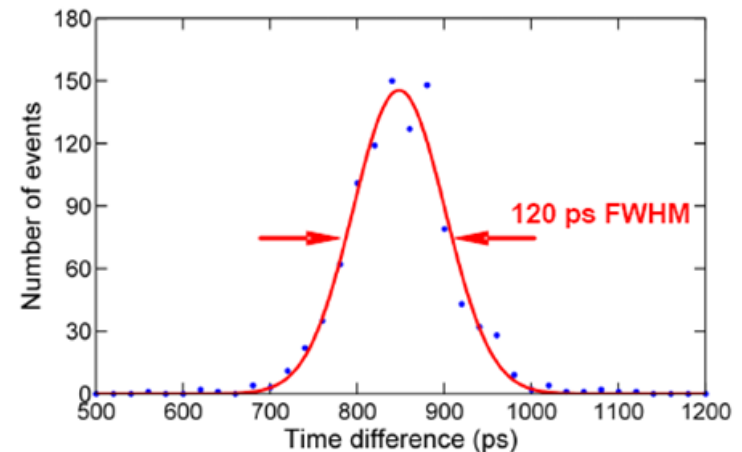
Analog Silicon Photomultiplier Detector

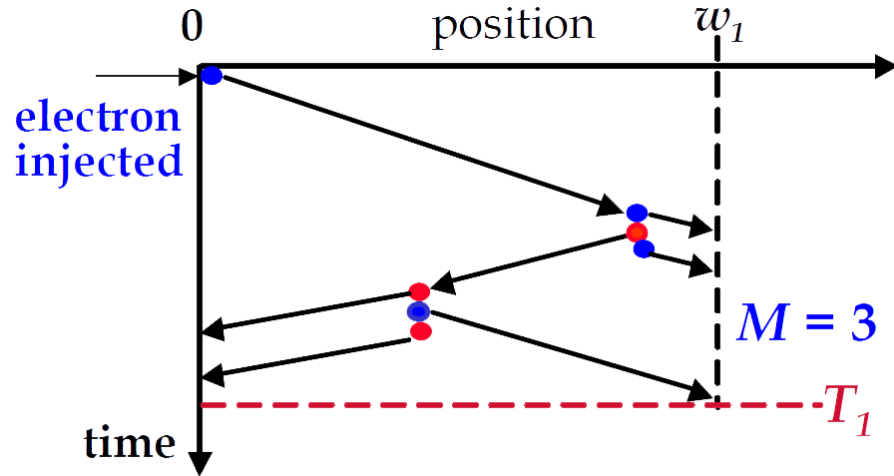


Digital Silicon Photomultiplier Detector

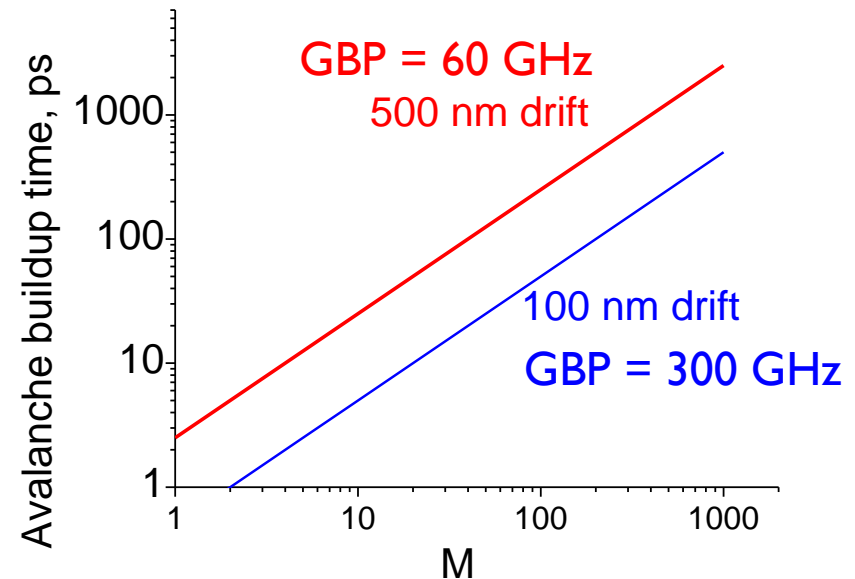


- Digital SiPM: each pixel contains its own electronics
- Low parasitic capacitance → reduced gain → improved stability





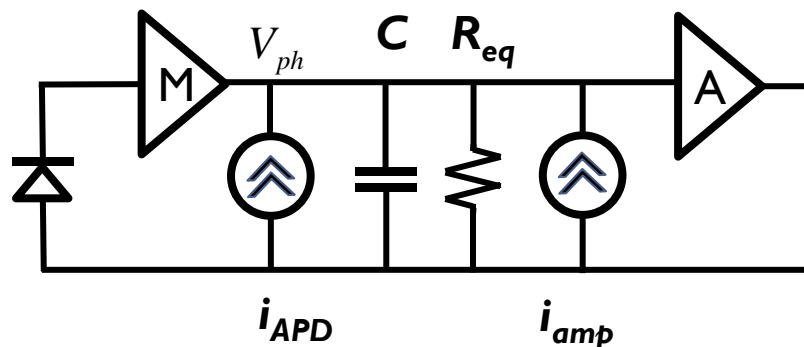
Avalanche buildup time for GaAs SAM APD



- Multiple transits in APDs reduce speed (multiplication buildup time)
- Geiger mode does not provide benefits
- Multiplication length can be reduced to $>100\text{nm}$ to increase speed
- Demonstrated **gain-bandwidth product** $\sim 300\text{-}400\text{ GHz}$



Fast APDs: S/N for single photoelectron detection



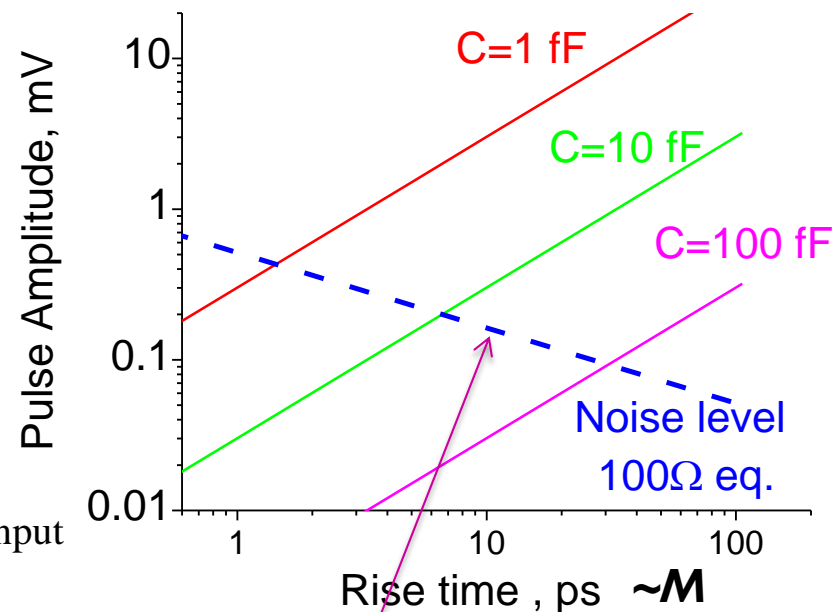
$$V_{ph} = \frac{I_{ph} \tau}{C} \xrightarrow{\text{single p.e.}} \frac{Me}{C} \quad R_{eq} C \ll \tau$$

$$v_{noise}^2 = 4\pi kTR_{eq} \Delta f$$

Dependent parameters:

- Fixed rise time τ limits **multiplication** M (fixed GBP)
- **Multiplication** M determines **total charge** at amplifier input
- **Signal voltage** determined by charging the **capacitor**
- **Noise** of an amplifier input determines **maximum capacitance**
- **Limited room for variations!**
 - Capacitances of ~ 10 fF are needed to obtain reasonable S/N ratio at low M 's
 - Need for low-C integration of the PD with amplifier \rightarrow **monolithic integration**

For single photoelectron
detection for GBP= 300 GHz



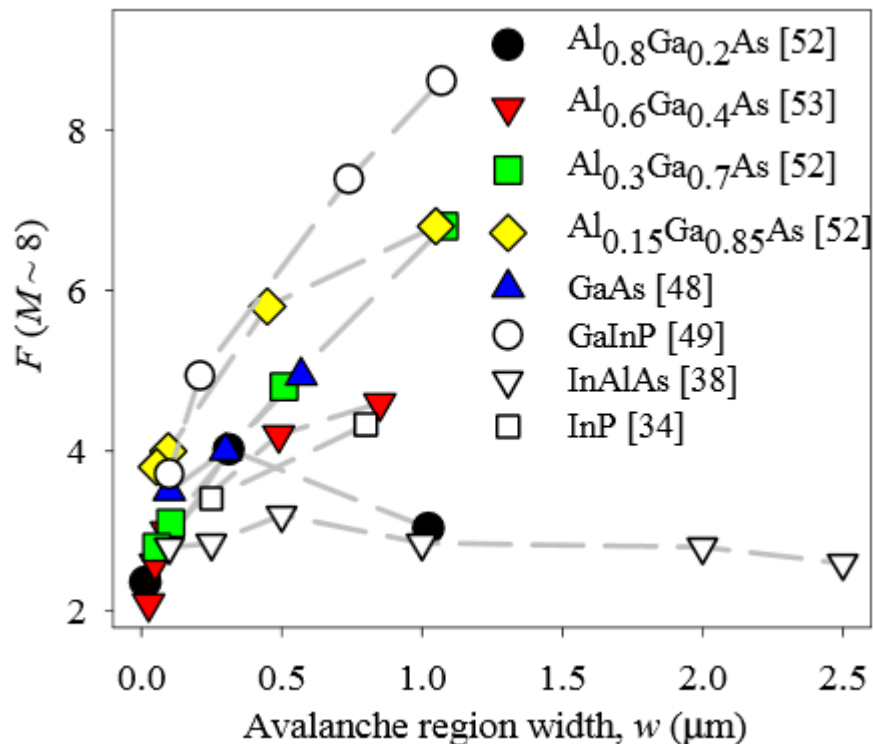
For S/N = 1:
M=20
C=20 fF



Improvement of APD noise: $\text{Al}_{0.8}\text{Ga}_{0.2}\text{As}/\text{GaAs}$

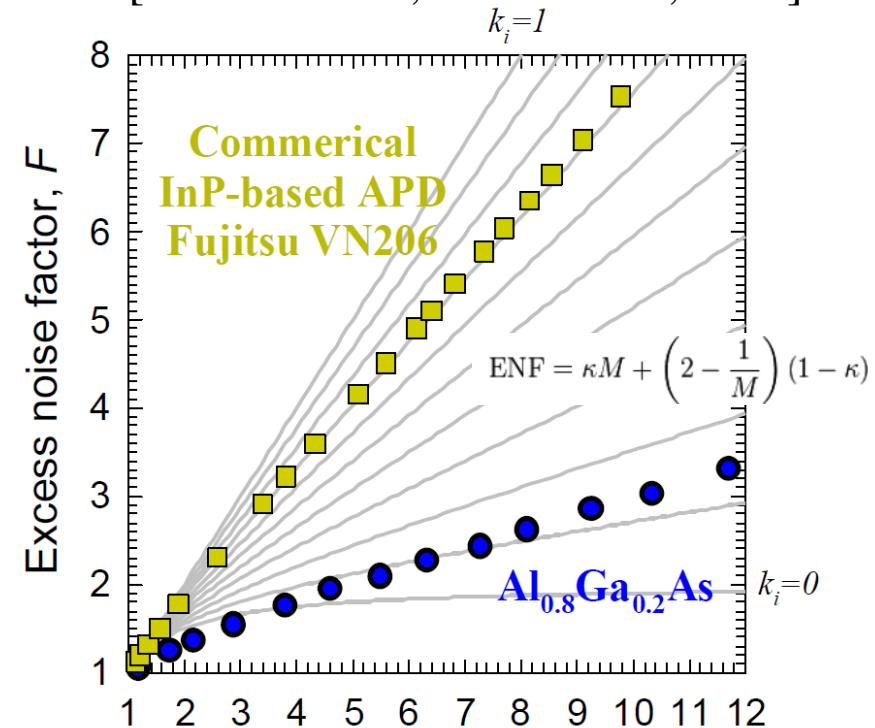
Excess noise in III-V APDs

[Xi, PhD thesis U. Sheffield, 2012]



Comparison of $\text{Al}_{0.8}\text{Ga}_{0.2}\text{As}$ and commercial InP APDs

[from J. David, U. Sheffield, 2003]

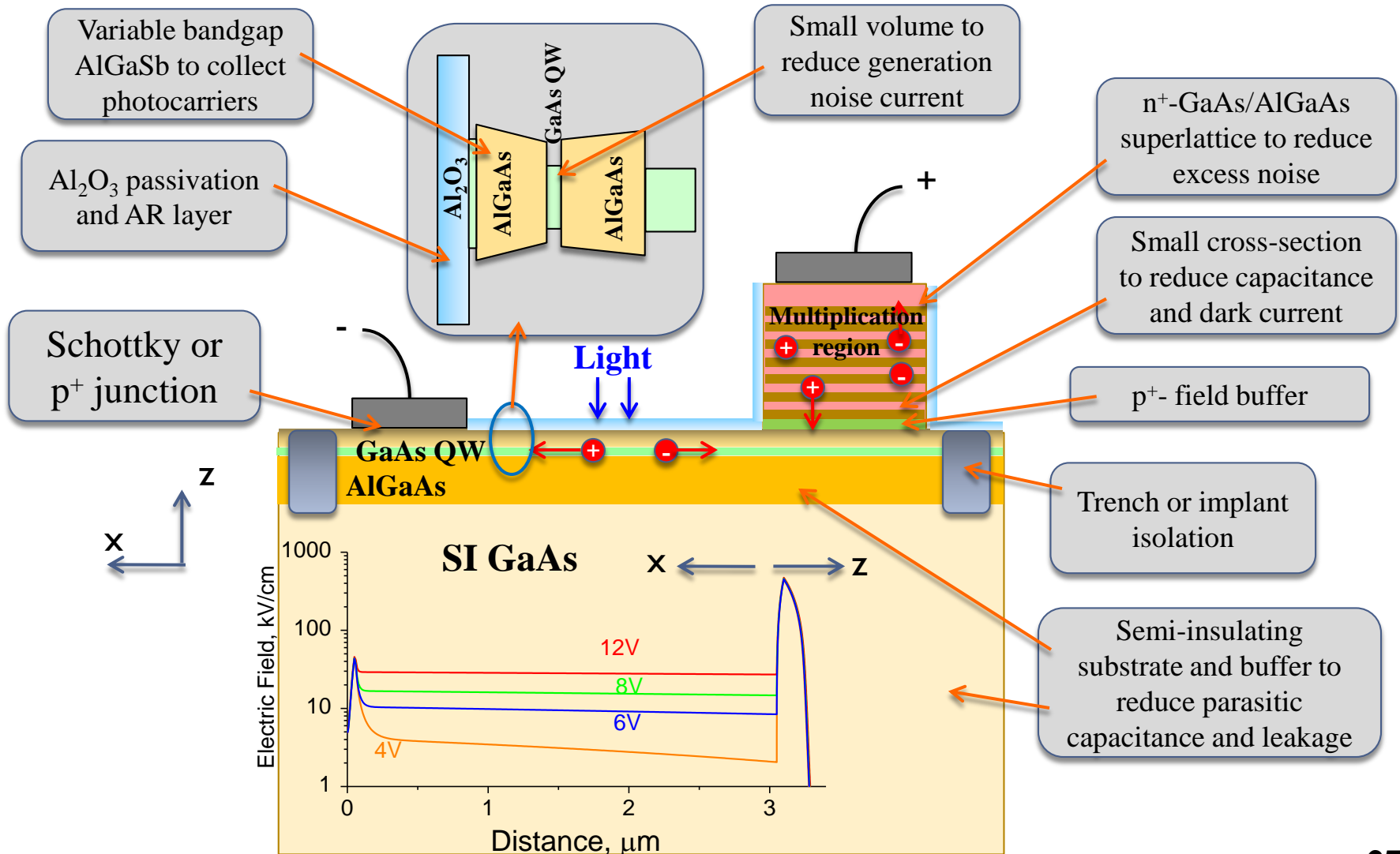


M

- Commercial InP-based APD give excess noise of $k_i \sim 0.7$
- Much lower excess noise can be obtained with wider bandgap III-V's, e.g. $\text{Al}_{0.8}\text{Ga}_{0.2}\text{As}$ as avalanche medium



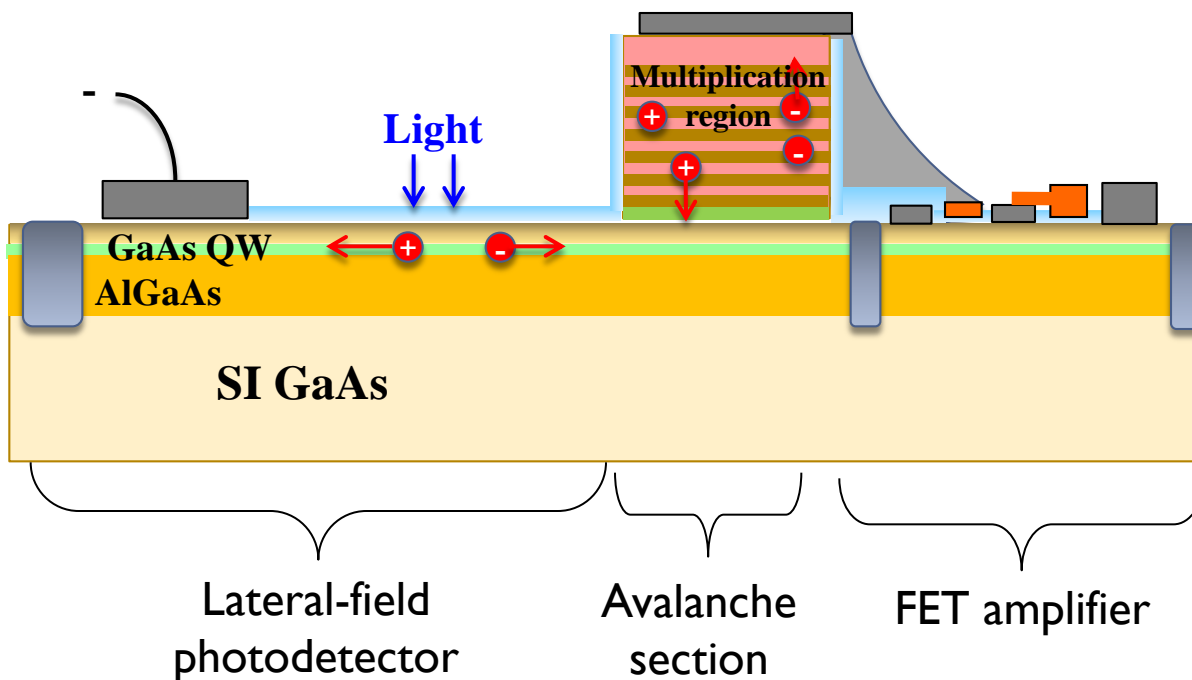
Concept for ps APD





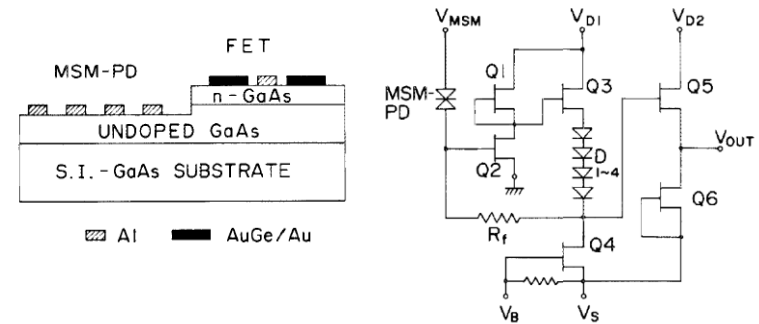
Integration with a transistor amplifier:

- FET uses same basic technology
- Possibly uses same QW as a photodetector
- Area separated by insulating trench or implant within the same pixel
- Integration of planar detector with FET previously demonstrated



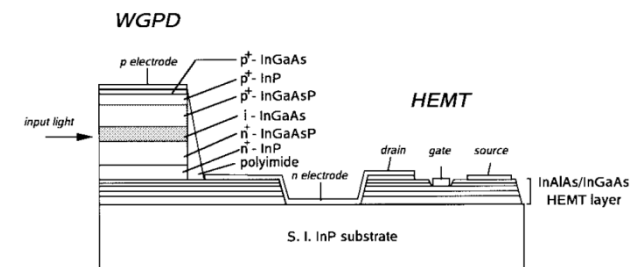
Integration of GaAs MSM with MESFET

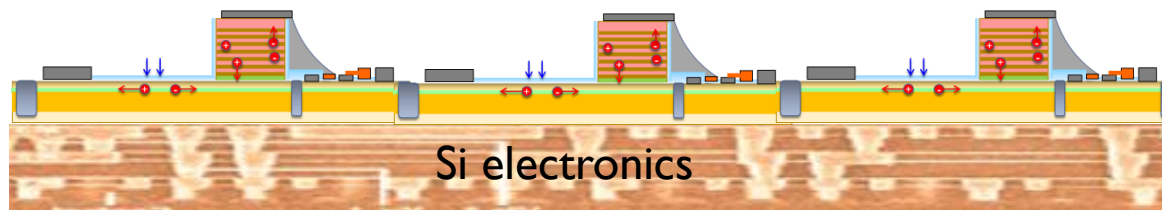
[Ito et al. APL 47 1129 (1985)]



Integration of InGaAs MSM with HEMT

[Kato, TMTT 47 1265 (1999)]

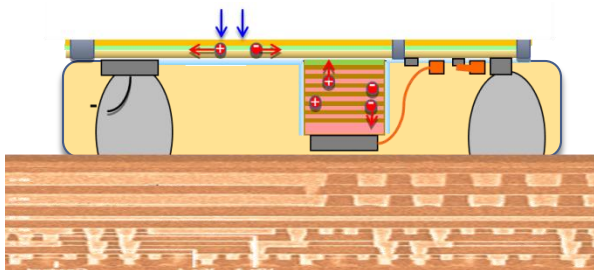




Finally: Partitioning and Integration with electronics (Si)

Face-up mounting of thinned GaAs wafer to Si

- Larger openings to run conductors to Si
- Still front side illumination
- Lost system area for electrical connections



Face down (flip-chip)

- Established technology using solder bumps, e.g. for FPAs
- Backfill with polymer for mechanical stability
- Minimizes interconnect problem
- Requires precise substrate removal: oxidation lift-off



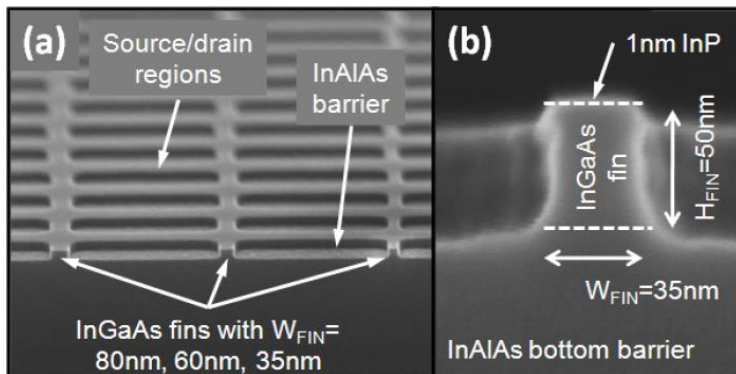
III-V Materials in Mainstream (Si) Electronics

III-V MOSFETs (and FinFETs) is extremely hot and fast developing topic pursued by many IC manufactures: INTEL, GlobalFoundries, IBM, TSMC, Samsung...

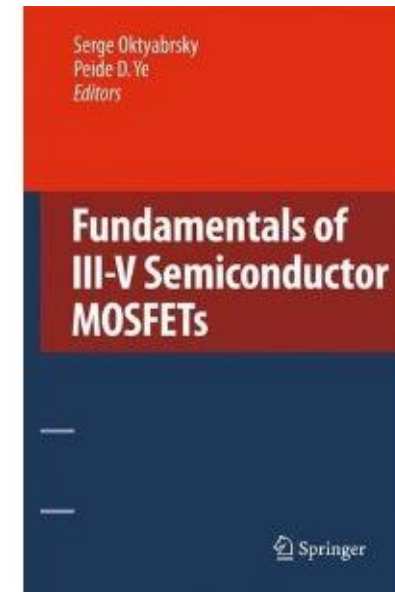
Tool manufactures (AMAT, TEL,...) and pilot IC R&D's (Sematech, IMEC) are adapting existing Si technologies / toolsets for III-V's



INTEL InGaAs FinFET (2010)



IMEC's InGaAs FinFET (2013)



2010

Si Industry - First III-V MOCVD Laboratory

Aixtron 300mm MOCVD tool for III-V on silicon processes

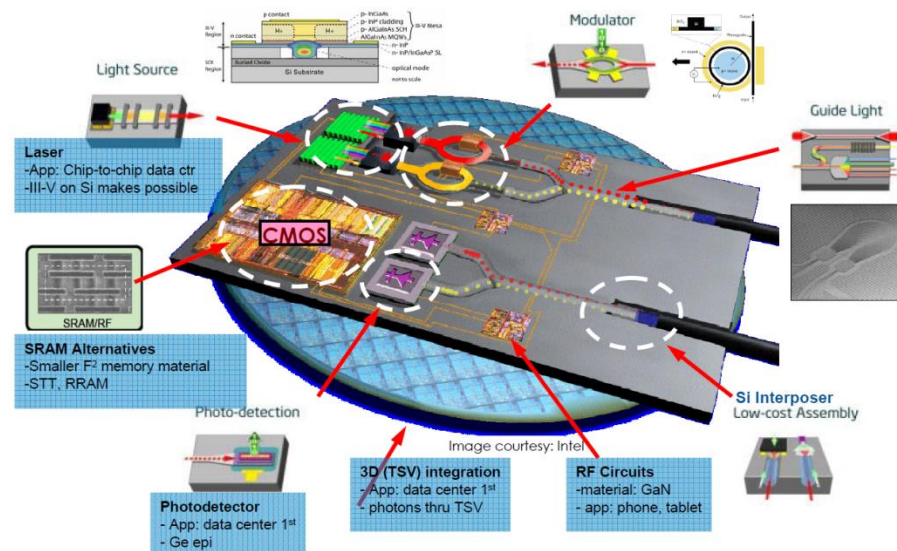


300 mm Si wafer and shower-head



**Integration on Si: from
R. Hill, Sematech 2013**

III-V and III-N on Si for beyond CMOS
Heterointegration of III-V materials enables advanced SOC



Aixtron G5 HT MOCVD* system
operated by SEMATECH and CNSE:

- III-As and III-N growths
- MO and hydride precursors
- In-situ cleaning

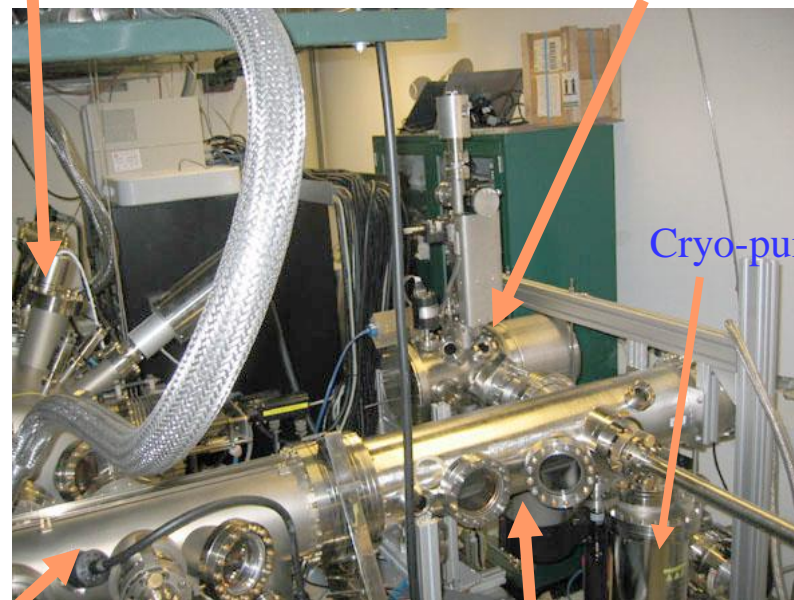
* MOCVD – metal-organic chemical vapor deposition



As MBE chamber



Sb-As MBE chamber



3x-magnetron chamber

Cryo-pump

MBE transfer module

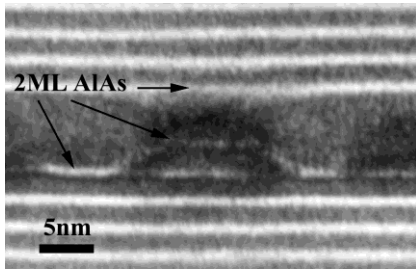
UHV transfer module

- MBE Veeco Gen II system:
 - Duo-chamber MBE system for As- and Sb- based III-V's
 - Triple-magnetron sputtering chamber (HfO_2 , TaN, TiW)
 - Reactive e-beam evaporator (HfO_2 and Al_2O_3)



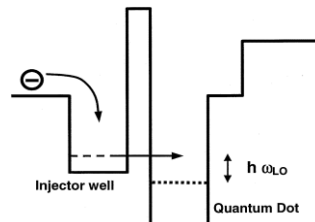
Compound Semiconductor Materials and Devices: Examples

Shape-engineered QD



Materials/Technologies

- MBE III-As and III-Sb
- Entire in-house processing
- Heterostructures
- In-situ (UHV):
 - High-k oxides
 - Contacts and Metallization

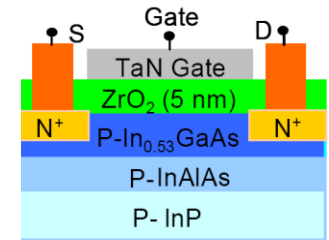
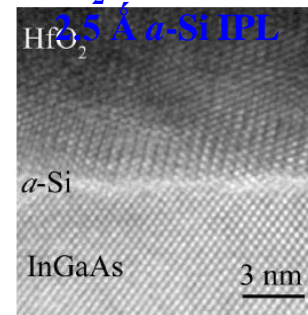


Electronic devices

III-V high-k MOSFETs

- In-situ high-k oxide for n-MOSFET
- High-mobility p-MOSFET
- Regrown source/drain

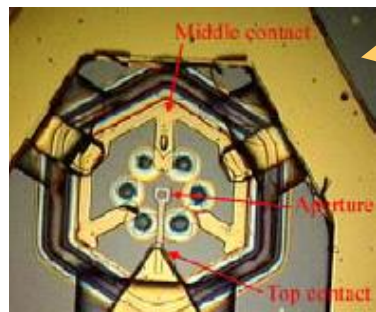
HfO₂/InGaAs with



Quantum dots – related application

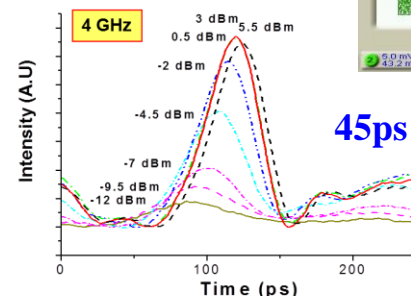
- Tunnel-coupled QD-QW VCSEL
- QD SLED for OCT
- Media with controlled photo-electron kinetics

VCSEL-Modulator

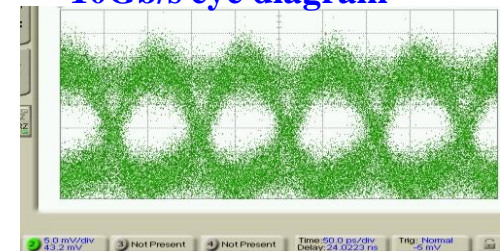


Photonic devices

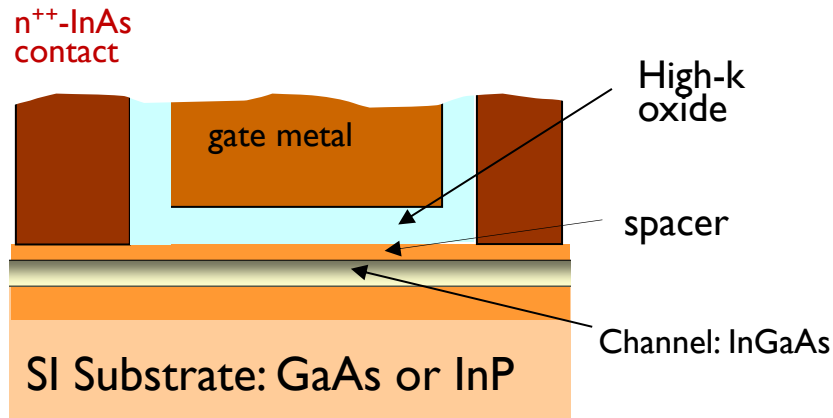
- Cavity optical decoupling approach: duo-cavity VCSEL-modulator
- Q-switching with intracavity modulator
- Bragg MQW lattice
- QWIPs/QDIPs
- QD solar cells



10Gb/s eye diagram

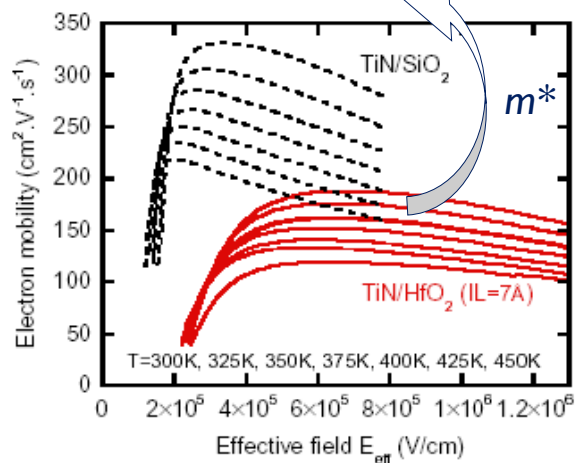


45ps FWHM Q-switch pulse generation



~8000-15000 $\text{cm}^2/\text{V}\cdot\text{s}$ in GaAs or InGaAs

~1500-2000 $\text{cm}^2/\text{V}\cdot\text{s}$ in GaAs or InGaAs



From Weber et al. SSE 2006

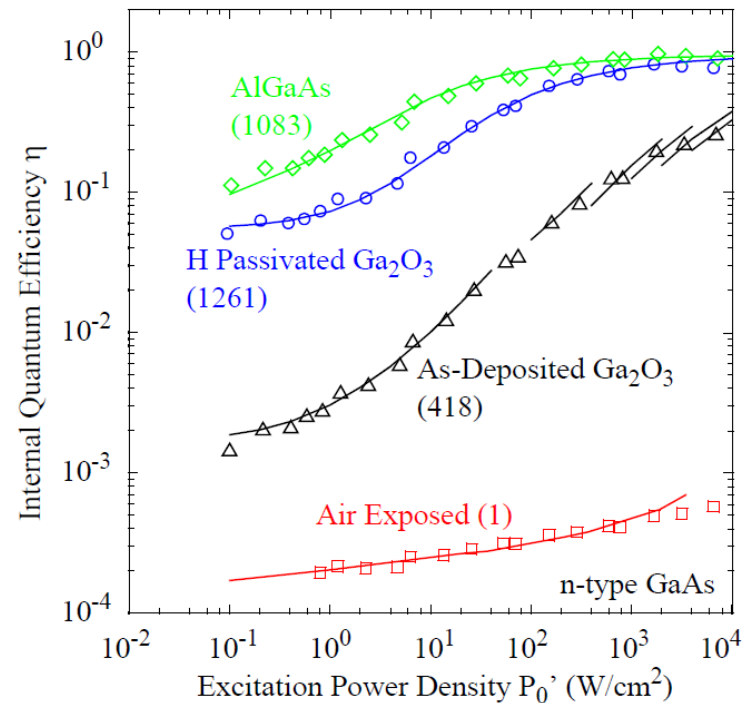
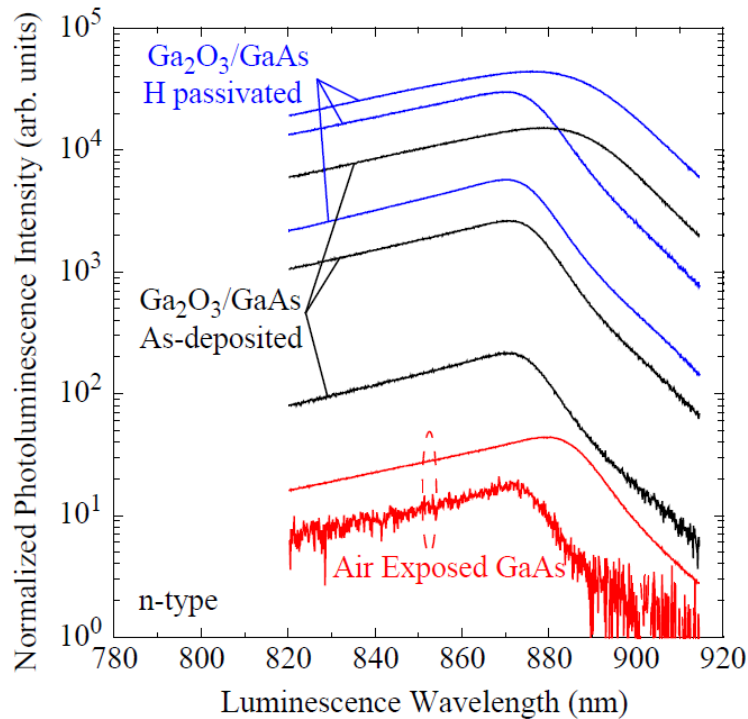
- **High quality interface with dielectric (as SiO_2/Si):**
 - Low surface recombination rate
 - Low density of interface states
 - High thermal and chemical stability of the interface
- **Improvement of channel transport:**
 - Low mass: Scattering – Coulomb, roughness, remote soft phonons
 - Buried channel
- **S-D resistance**
 - Regrown InAs for n-type or InSb on p-type
 - Epi-SD and gate-last flow



GaAs/high-k Interfaces: Surface recombination

RT Photoluminescence and Internal Efficiency of GaAs with Different Surfaces

[Passlack, in “Materials Fundamentals of Gate Dielectrics...” 2005]



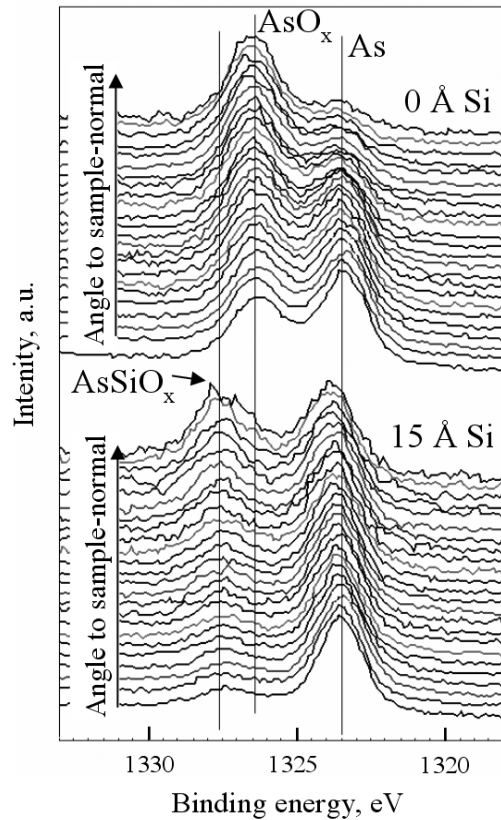
- Air exposed surface has high recombination velocity \rightarrow kills photocarriers
- Great (~4-5 orders) reduction of the surface recombination demonstrated with various passivation techniques



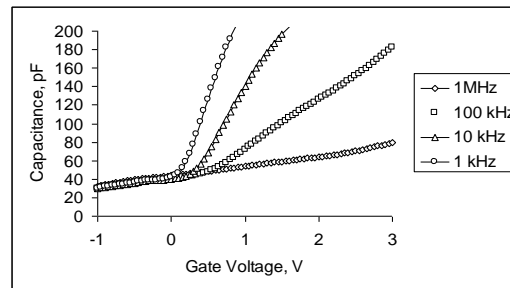
a-Si Interface Passivation of High-k/GaAs interface

1.5 nm a-Si on GaAs + PVD HfO₂

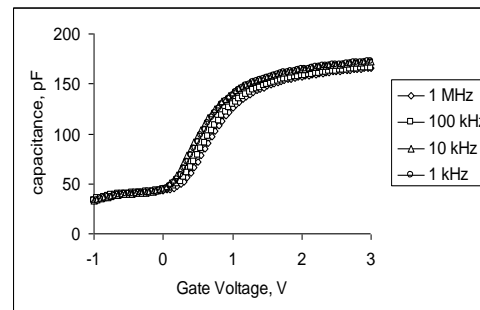
Angle-resolved As 2p XPS spectra and CV's



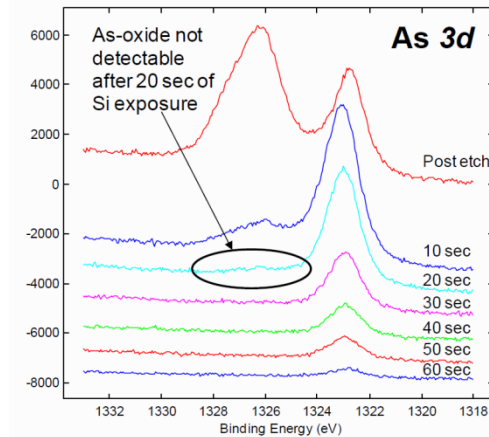
Fermi level is pinned



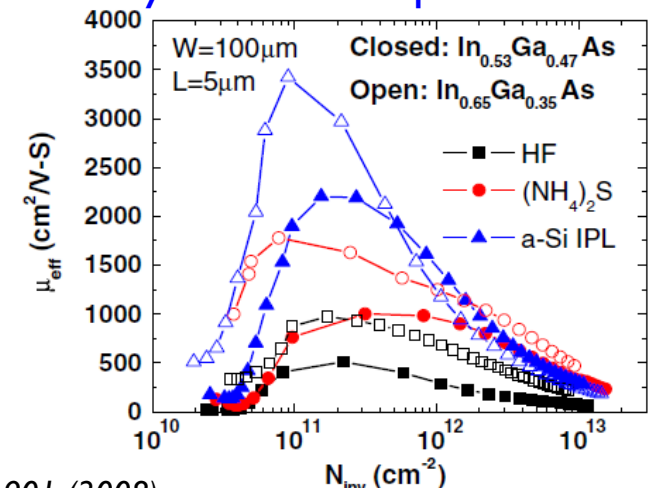
Fermi level is not pinned



Wallace and Vogel groups, UTD
Removal of As-O with a-Si deposition



Eff. mobility vs. different passivation

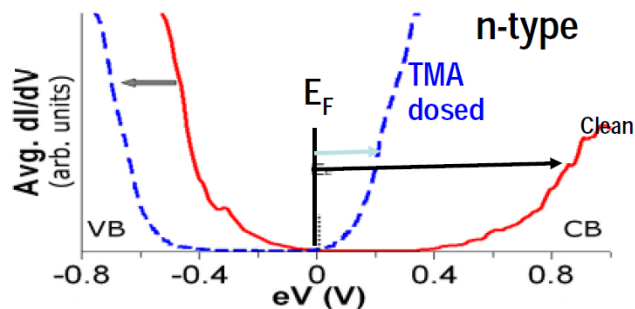
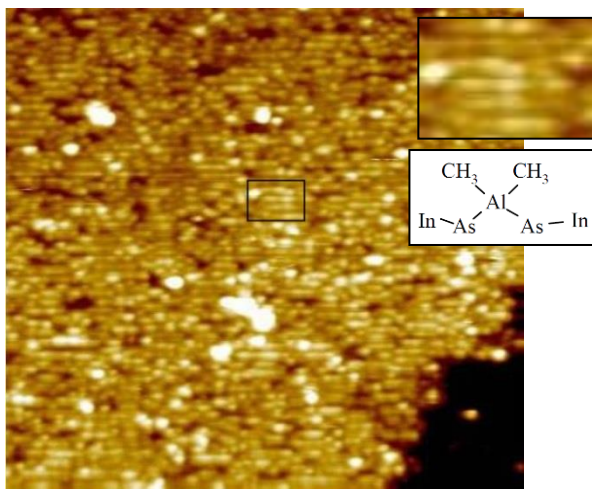


Koveshnikov, APL 88, 022106 (2006)
Oktyabrsky, Mat. Sci. Eng. B, 135 272 (2006)

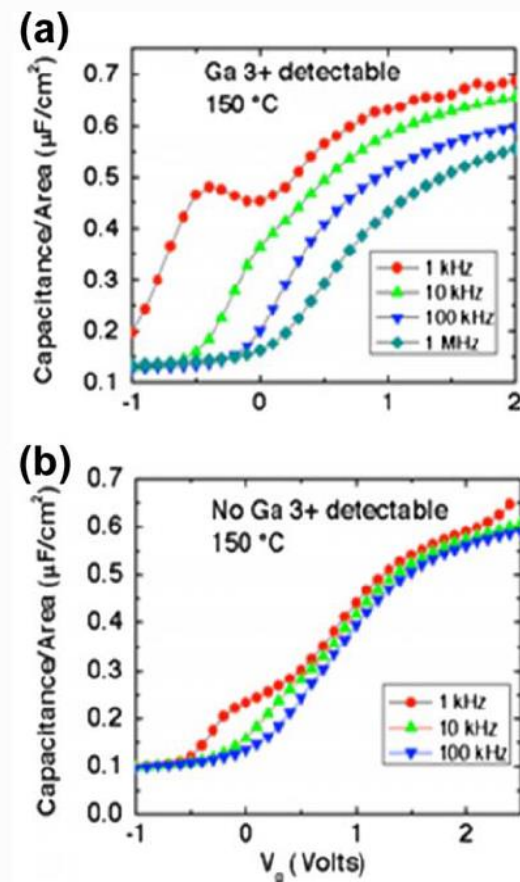
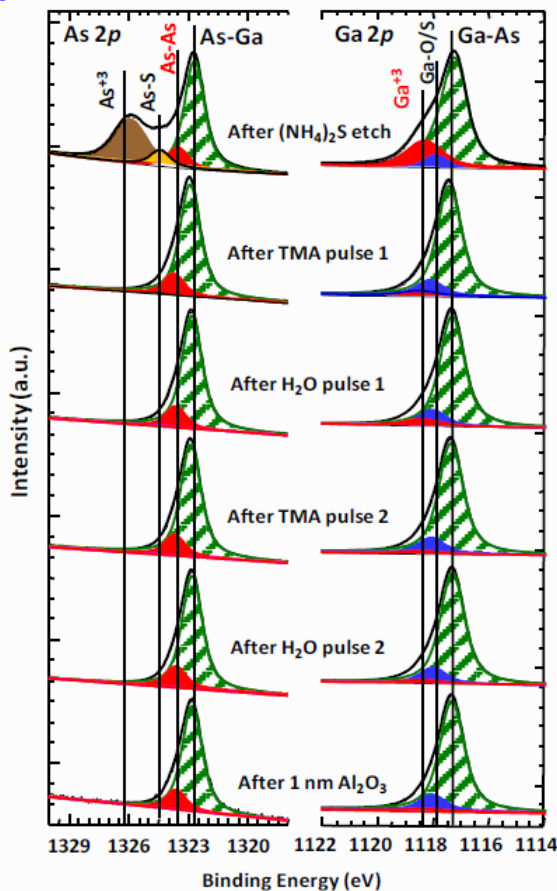
Hinkle, APL 92, 071901 (2008)
Milojevic, APL 93, 202902 ; 252905 (2008)
Sonnet, Microel. Eng. 88, 1083 (2011)



UHV STM and STS of TMA-exposed InGaAs surface (Kummel group, UCSD)



In-situ XPS and C-V (Wallace and Vogel groups, UTD)

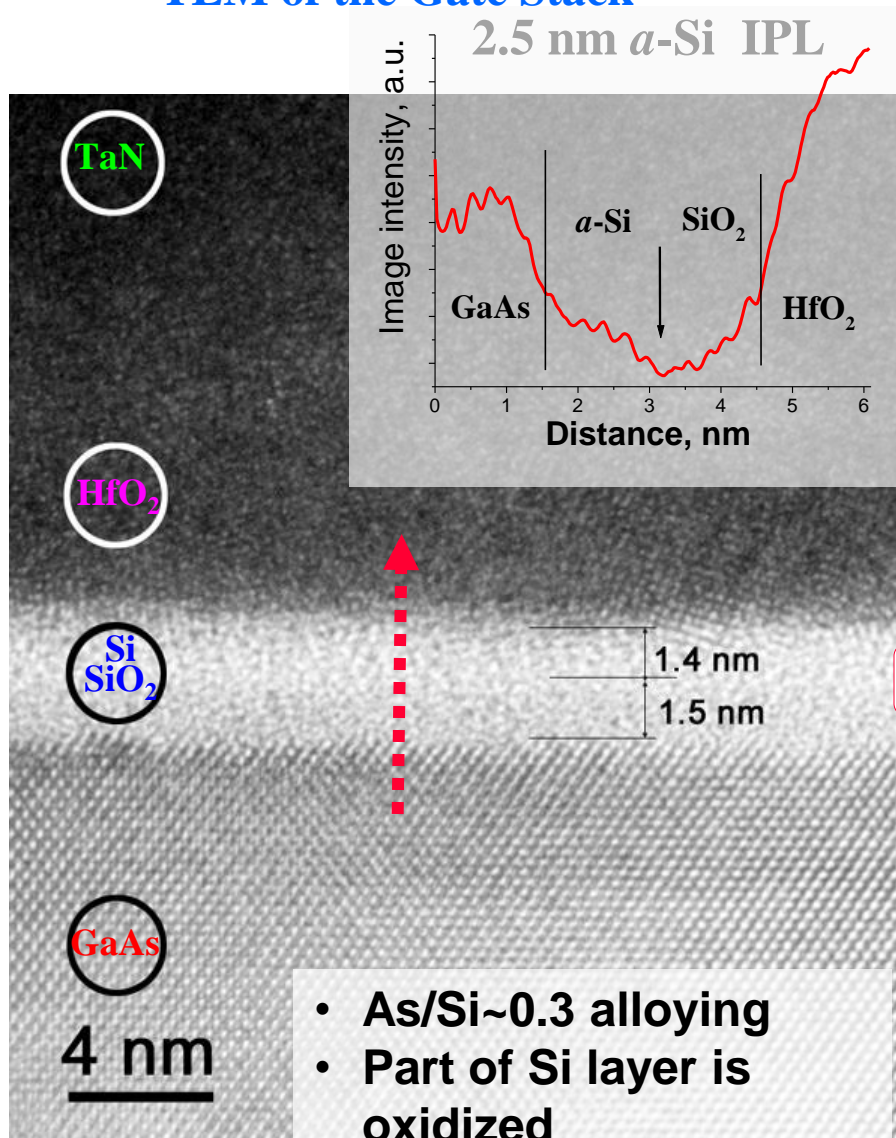


- Saturation dose of TMA results in a near monolayer coverage with no substrate atom displacement
- TMA dosing restores the Fermi level to the CB edge

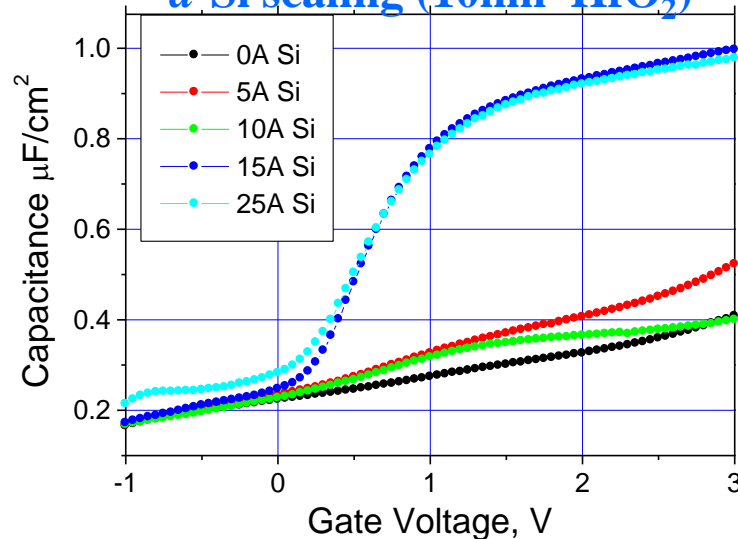
- TMA is efficient to remove Ga- and As-oxides
- As-As dimers is the major component left



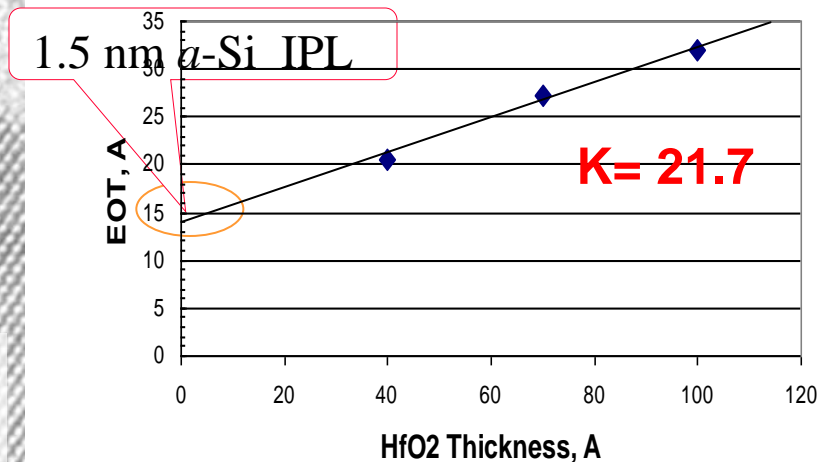
TEM of the Gate Stack



a-Si scaling (10nm HfO₂)



HfO₂ scaling (1.5 nm *a*-Si)



• The k-value of the HfO₂ gate oxide ~21-22 38



III-V Processing

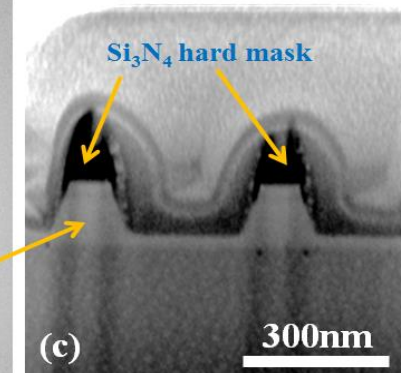
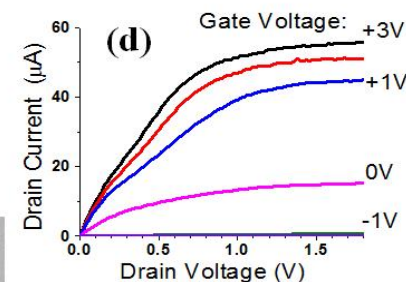
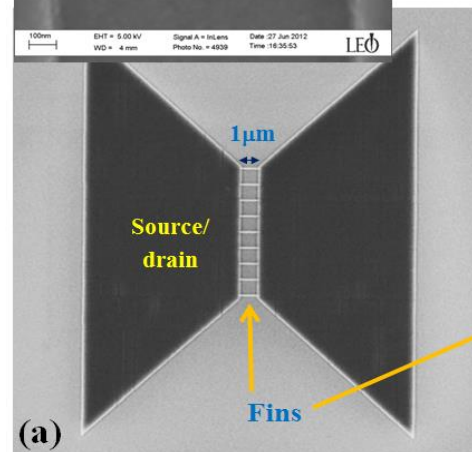
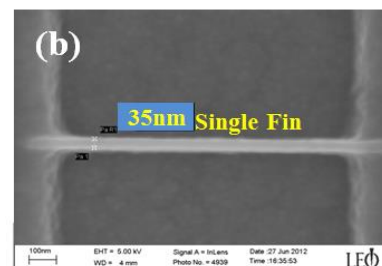
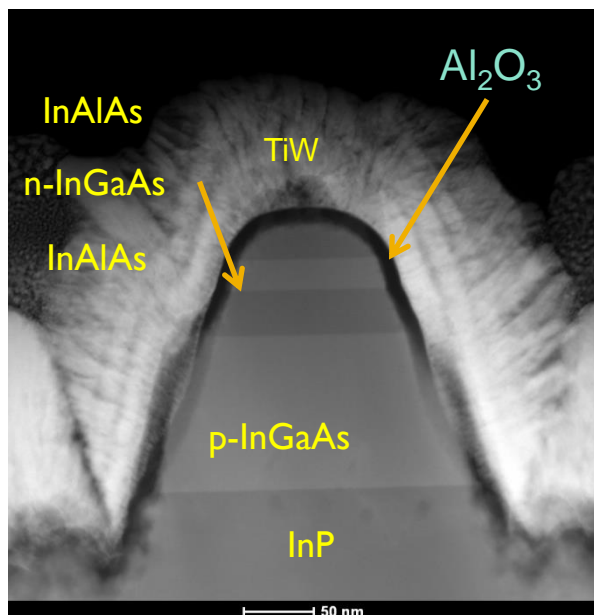
E-beam lithography process for FinFET fabrication

E-beam exposure using Vistec VB 300

- NEB and HSQ negative resists: Fin Width down to 50 nm

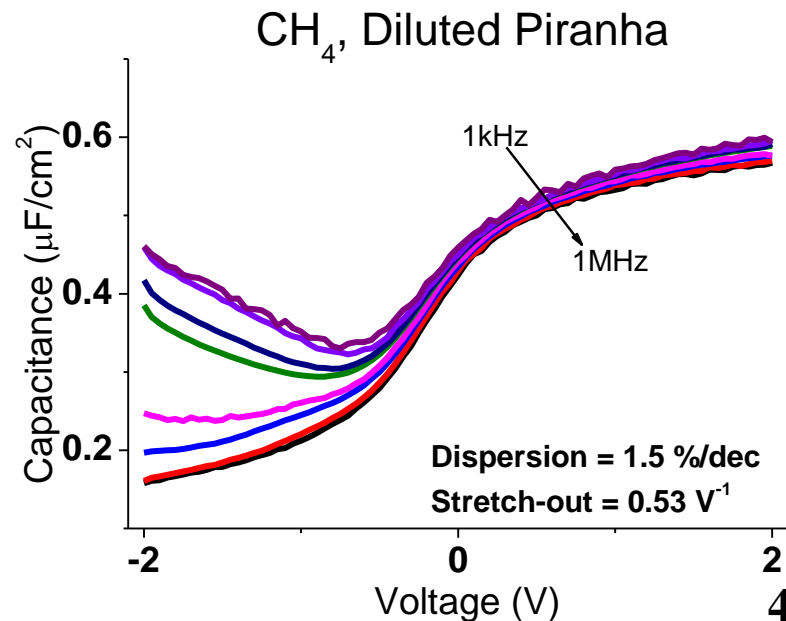
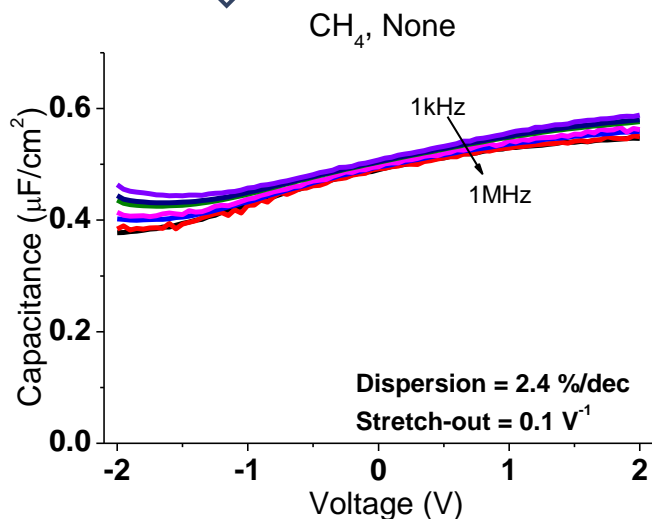
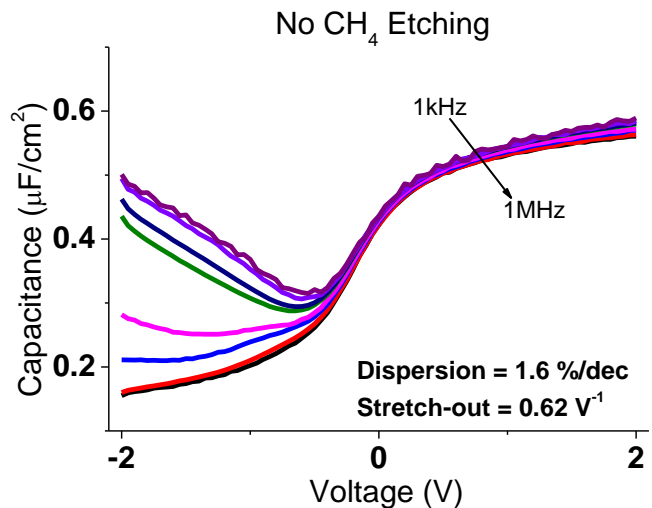
Plasma etching of hard mask pattern into InGaAs

- $\text{CH}_4/\text{H}_2/\text{Ar}$ recipe optimized for smooth, vertical sidewalls
- Damage removal with diluted piranha wet etch





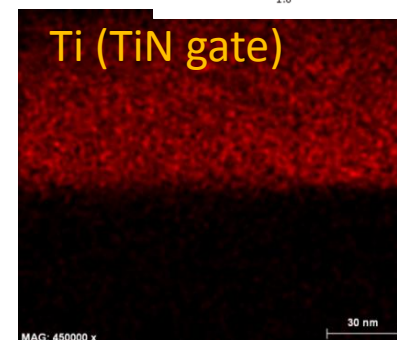
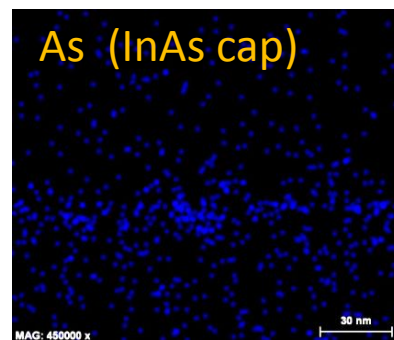
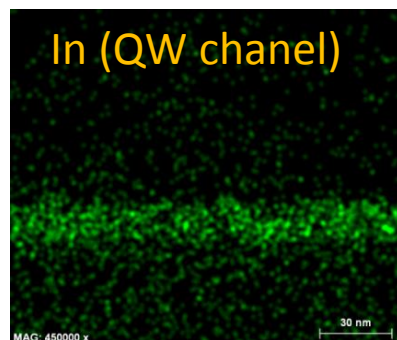
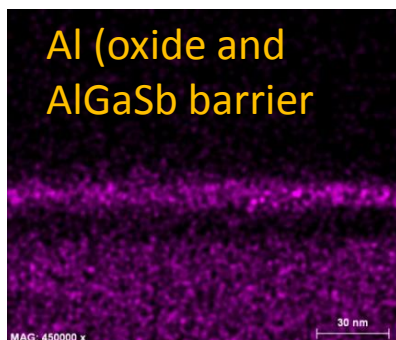
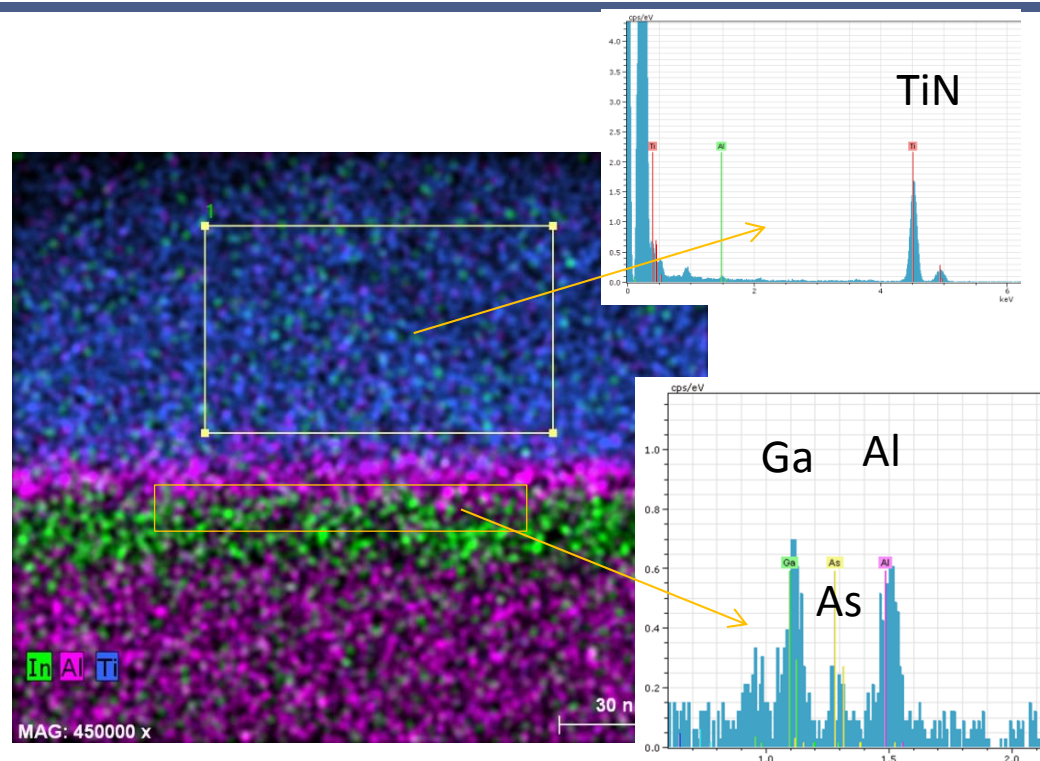
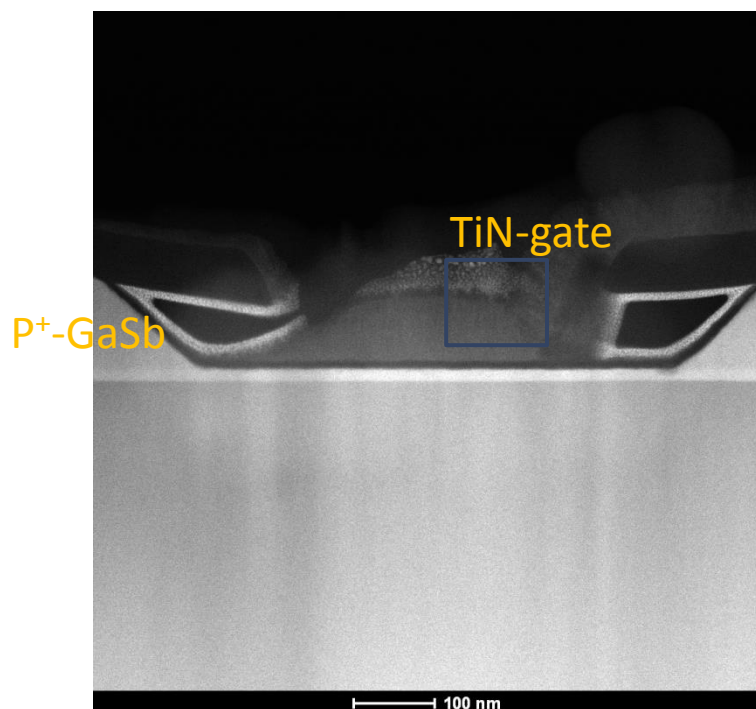
Ion Damage Removal



RIE damage removal after CH₄/H₂/Ar etch

- 1 μm n-In_{0.53}GaAs on n-GaAs MOS Capacitor
- Diluted Piranha = similar CV to as-grown surface
- CV characteristics restored

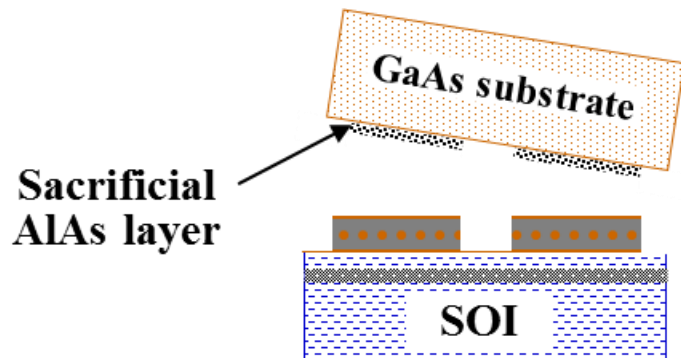
STEM/EDX of gate-last MOSFET



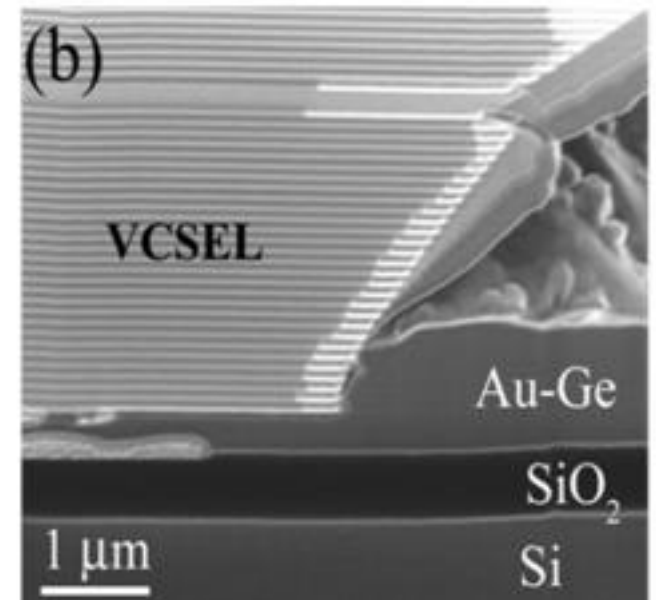
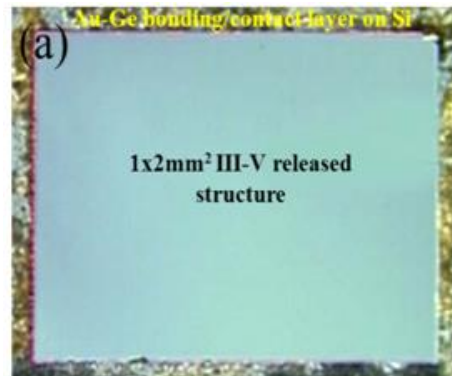
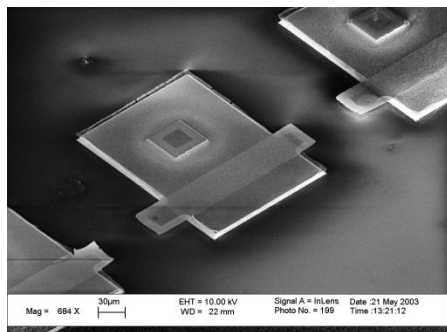
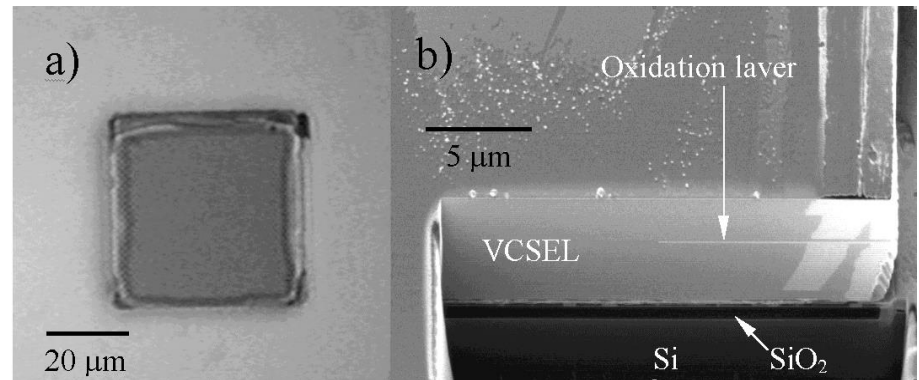
- Gate-last flow MOSFET with epi p⁺-GaSb SD and InAs etch stop layer
- After TMAH recess etch, InAs (1.5nm) is present on the surface

Oxidation Lift-off Technology

Oxidation lift-off



FIB cross-sections of the device fabricated by oxidation lift-off technique.



- Bonding by Au-Ge eutectic or polymer
- Bonding, device separation and formation of the oxide isolation in the same process



Conclusions

- Group III-V technologies are rapidly progressing towards mainstream logic ICs
- III-V materials have credible benefits for photodetectors:
 - High carrier velocity,
 - Low saturation field
- Planar lateral field architecture is beneficial for fast UV PD
 - Low capacitance
 - Transport close to the surface
 - Reduced volume for current
- Materials benefits + Available technologies \Rightarrow ps PDs ?



Acknowledgements

CNSE students

- Alex Varghese
- Rama Kambhampati (GF)
- Andrew Greene
- Shailesh Madiseti
- Thenappan Chidambaram

CNSE Staff

- Michael Yakimov
- Vadim Tokranov
- Shun Sasaki

Funding:

- NSF
- AFOSR
- SRC
- INTEL
- GLOBALFOUNDRIES

Academia collaborators

- Peide Ye (Purdue)
- Jesus del Alamo (MIT)
- Jack Lee (UTexas at Austin)
- Darrel Schlom (Cornell)
- Nikolai Faleev (Arizona State)

Industrial collaborators

- Sergei Kovesnikov (Intel)
- Dmitry Veksler (Sematech)
- Niti Goel (Intel)
- Ajey Jacob (GF)
- Steven Bentley (GF)

Many thanks to FNAL

- Pavel Murat
- Erik Ramberg